DACHER: An Energy-Saving Dynamic Region Cluster-Head Election Routing Protocol for Wireless Sensor Networks

Xiaohu Huang, Bing Han, Dezhi Han, *Senior Member, IEEE*, Ruyue Zhang, and Kuan-Ching Li, *Senior Member, IEEE*

***Abstract*—Wireless sensor networks (WSNs) underpin numerous industrial Internet of Things (IoT) applications, yet their operational lifetime is severely curtailed by the rapid emergence of energy holes around heavily loaded nodes. To address this critical issue, we present a dynamic area cluster-head election routing (DACHER) protocol that equalizes network-wide energy consumption through three mutually reinforcing mechanisms. Spatially, ring-based (RB) partitioning stratifies the network into concentric annuli to radially distribute load. An energy-aware periodic rotation (PR) scheme temporarily reallocates the cluster-head (CH) burden according to residual energy E_j and rotation angle β, pre-empting hot-spot formation. For routing, relay-assisted (RA) chained forwarding replaces energy-intensive, long-haul transmissions with efficient, short-range multihop links, markedly reducing the communication cost for distant CHs. The synergy of these spatial, temporal, and routing strategies extends both the stability period length (SPL) and last node death (LND) lifetime. Comprehensive simulations on networks of 200–1000 uniformly distributed nodes validate our approach. At the 1000-node scale, DACHER achieves an average LND of 1655 ± 49 rounds (95% CI: 1553–1757) and prolongs the SPL by 96–516 rounds, outperforming contemporary protocols like Weighted K-means based LEACH-C (WLEACH-CK), load-aware CH rotation (LAR-CH), layered-based routing (LBR)-gray wolf optimization (GWO), and combining election and routing among cluster heads (CER-CH) by 5%–29%. These gains translate into lower per-round control overhead and higher overall energy efficiency. Altogether, DACHER provides a lightweight, scalable solution that substantially extends the longevity of large-scale WSNs composed of stationary, energy-homogeneous nodes without sacrificing algorithmic simplicity.**

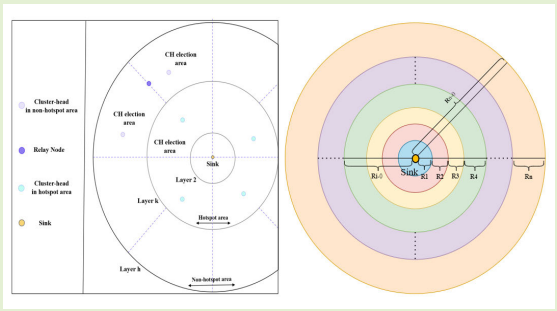

***Index Terms*— Cluster head (CH), Internet of Things (IoT), last node death (LND), stability period length (SPL), wireless sensor networks (WSNs).**

Received 8 March 2025; revised 25 April 2025, 26 May 2025, and 25 June 2025; accepted 14 July 2025. Date of publication 24 July 2025; date of current version 3 September 2025. This work was supported in part by the Natural Science Foundation of Fujian Province of China under Grant 2022J011128, in part by the Natural Science Foundation of Shanghai under Grant 25ZR1401156, in part by Shanghai Science and Program of Shanghai Academic/Technology Research Leader under Grant 23XD1431000, and in part by the Top-Notch Innovative Talent Training Program for Graduate Students of Shanghai Maritime University under Grant 2022YBR010. The associate editor coordinating the review of this article and approving it for publication was Prof. Reza Malekian. *(Xiaohu Huang and Bing Han are co-first authors.) (Corresponding authors: Bing Han; Kuan-Ching Li; Dezhi Han.)*

Xiaohu Huang, Dezhi Han, and Ruyue Zhang are with the College of Information Engineering, Shanghai Maritime University, Shanghai 201308, China (e-mail: hxhinfinite@163.com; dzhan@shmtu.edu.cn; zhangry1228@163.com).

Bing Han is with the College of Physics and Electronic Information Engineering, Minjiang University, Fuzhou 350108, China, and also with Shanghai Ship and Shipping Research Institute Company Ltd., Shanghai 200135, China (e-mail: han.bing@coscoshipping.com).

Kuan-Ching Li is with the Department of Computer Science and Information Engineering, Providence University, Taichung 43301, Taiwan (e-mail: kuancli@pu.edu.tw).

Digital Object Identifier 10.1109/JSEN.2025.3590485

NOMENCLATURE

Notation	Description
d	Distance.
k	Data packet size in bits.
$E_{\text{tx}}(k,d)$	Energy consumed for transmitting k-bit data over d-distance.
E_{elec}	Energy consumed to transmit one bit of data.
$E_{\text{Rx}}(k)$	Energy consumed for receiving k-bit data.
ε_{fs}	Amplifier characteristics of the free-space channel.
ε_{mp}	Amplifier characteristics of the multipath channel.
E_{DA}	Energy consumed for aggregating data.
R	Maximum coverage communication range.
$\text{CH}(j)_{\text{score}}$	Scoring function of CHs.
$R(k)_{\text{score}}$	Scoring function of relay nodes.
$D_{\max}$	Half of the chord length subtended by the outer boundary arc of the CH electoral area.

D_j Vertical distance between the node and the centerline of the election area.
E_0 Initial energy of a sensor node.
N_{nb} Neighbors of the sensor node.
r_0 Initial radius of the first layer.
R_i Width of the circular region of layer.

I. Introduction

THE Internet of Things (IoT) is now a cornerstone of data-driven innovation, with the installed base of connected devices projected to exceed 41.6 billion and to generate 79.4 ZB of data by 2025 [1], [2]. Wireless sensor networks (WSNs) form a critical, low-power tier within this large-scale infrastructure: they harvest fine-grained environmental data and relay it to upper layer platforms for real-time analytics and control.

A typical WSN relies on multihop, short-range links among randomly deployed sensor node (SN), which forward their measurements to a centrally located base station (BS) endowed with ample energy and external-network connectivity [3]. Because each sensor node operates on a finite, usually non-rechargeable battery, network longevity hinges on judicious energy management; extending node lifetime has become a primary research imperative [4].

Currently, clustering is a widely adopted and efficient topology management method in WSNs, initially introduced to balance energy consumption across the network [5]. Applying clustering techniques in this context enhances network efficiency and energy management. Fig. 1 illustrates the clustering context in WSNs, where sensor nodes exchange information and transmit data to the BS. Clustering involves partitioning the network into multiple clusters, each managed by a cluster head (CH). The CH collects, processes, and forwards data from the member nodes (MNs) to the BS. The optimal CH is selected based on various parameters, and reclustering is performed when the CH's energy falls below a specific threshold to maintain network reliability.

Clustering protocols in WSNs typically hinge on CH election, cluster formation, and data forwarding. The seminal LEACH scheme [6] elects CHs via a probabilistic threshold, cyclically rotating the role to distribute load. Yet, this random selection disregards node location and residual energy, creating pronounced inefficiencies. Because radio energy dissipation scales with distance as d^n (with $n \in [2, 4]$), a CH located at twice the distance to the BS compared with another can incur a fourfold–16-fold increase in transmission-energy expenditure, hastening the premature exhaustion of outlying nodes. The centralized variant LEACH-C [7] mitigates this spatial bias by invoking a simulated-annealing optimizer at the BS to nominate energy-balanced CHs. However, its global coordination incurs a prohibitive overhead: every node must report its state to the BS in each round, yielding $O(n)$ control traffic and attendant energy cost. Even with this "optimal" CH set, the dominant limitation persists—the high amplifier energy required for single-hop, long-range transmissions to the BS ultimately caps the network's lifetime.

To mitigate load imbalance, Tang and Han [8] proposed multi-base station clone detection (MSCD), which partitions

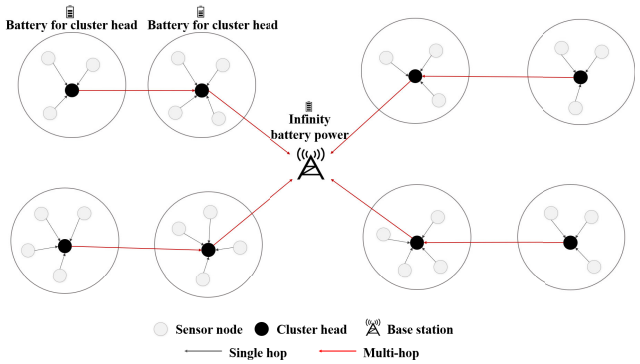

Fig. 1. Clustering architecture demonstration.

the network into concentric rings and employs a chained inter-cluster path. MSCD delivers measurable gains—sustaining a 98.6% clone-detection rate even with 10% malicious nodes—yet its analysis reveals a secondary bottleneck: when the detection task is executed more than ten times per round, energy expenditure in the relaying non-hot-spot rings rises sharply, shifting the hot spot from the center to the periphery. Later studies attempt to rectify this residual imbalance. Benelhouri et al. [9] introduce evolutionary gateway-based load-balanced routing (E-GLBR), a genetic-algorithm framework that balances residual energy, hop distance, and node density, whereas Wang et al. [10] present unequally clustered routing protocol based on multihop threshold distance (UCRTD), which derives analytical threshold distances to forge unequal clusters and lighten the load on inner ring nodes. Despite their progress, both approaches entail trade-offs: evolutionary optimization imposes nontrivial computation overhead on resource-constrained motes, while unequal-cluster architectures remain largely static and thus slow to adapt to bursty traffic. In short, without a lightweight, energy-aware dynamic mechanism that cyclically re-elects CHs and relay nodes across all rings, some region—central or peripheral—inevitably becomes an energy sink. This gap motivates the cyclic-rotation paradigm embedded in dynamic area CH election routing (DACHER), whose periodic reassignment equalizes load network-wide and forestalls premature regional failures.

To overcome the limitations, we propose DACHER, a lightweight clustering protocol that couples ring-based (RB) partitioning with dynamic CH rotation to achieve sustained load balance. Compared with the MSCD, WLEACH-CK, UCRTD, and related protocols, our design offers clear performance advantages, as evidenced by a comprehensive literature comparison. Unlike passive schemes, DACHER performs a proactive, periodic rotation (PR) of annular sectors, forestalling the emergence of local energy hot spots. Transmission inefficiencies are mitigated by a relay-assisted (RA), chained multihop backbone that shields distant CHs from high long-haul energy costs. Because this cyclic rotation relies solely on locally cached geometric information, DACHER substantially curtails the frequency and scope of the costly, network-wide CH-election handshakes typical of conventional schemes, resulting in meaningful energy savings. Extensive simulations confirm that these architectural advantages

translate into substantial, quantifiable gains in stability period, network lifetime, and per-round energy efficiency. The principal contributions are fourfold.

1) *Ring-Layer Partitioning for Balanced Clustering:* Instead of random or grid-based clustering, DACHER segments the sensing area into concentric rings. Each layer covers an appropriate radial distance to the BS, minimizing localized hot spots and over-competition among nodes close to the BS.
2) *Relay-Node Chaining in Non-Hot-Spot Regions:* In outer rings, DACHER introduces carefully selected relay nodes that form multihop communication links among clusters. This reduces direct transmissions to the BS, alleviates energy burdens on distant CHs, and improves overall load balancing.
3) *PR of Annular Sectors:* By incrementally rotating the ring boundaries around the BS, DACHER reassigns cluster membership over time. This mechanism prevents the same nodes from repeatedly serving as CHs and mitigates premature energy depletion, extending the stability period and overall network lifetime.
4) *Quantifiable Gains in Lifetime and Stability:* In 1000-node deployments, DACHER sustains network operation for 2048 rounds, compared with 1587–1945 rounds achieved by WLEACH-CK, load-aware CH rotation (LAR-CH), layered-based routing (LBR)-gray wolf optimization (GWO), and combining election and routing among cluster heads (CER-CH)—representing a 5%–29% improvement in last node death (LND). It also prolongs the stability period length (SPL) by 96–516 rounds under the same configuration, effectively deferring energy-hole formation and demonstrating superior load-balancing robustness.

The rest of this article is organized as follows. Section II describes the related works, while the network model and the system modeling are described in Section III. Then, in Section IV, the proposed algorithm is presented in three key operational stages: the rotating mechanism, clustering algorithm, and energy-consumption calculation. Next, in Section V, the experimental results and performance analysis are demonstrated. Finally, conclusions and directions for future work are depicted in Section VI.

II. Related Work

A. Clustering

In the clustering method for WSNs, sensor nodes are grouped into clusters, each managed by a designated CH. The CH is responsible for gathering intracluster information, processing data fusion, and forwarding data to other clusters or the BS [11]. Upon selection, the CH broadcasts its status to surrounding nodes, prompting MNs to join based on signal strength. MNs send join requests to the CH, which then allocates time-domain multiple access (TDMA) slots for efficient data transmission.

As illustrated in Fig. 2, during the intracluster transmission phase, all nodes transmit data to the CH according to the TDMA schedule. The CH, then, aggregates this data and sends the processed information to the BS, directly or via multihop routing. Intercluster transmission relies on a network of CHs to handle long-distance data routing. MNs can often deactivate their communication modules, simplifying their operations and reducing network traffic [12].

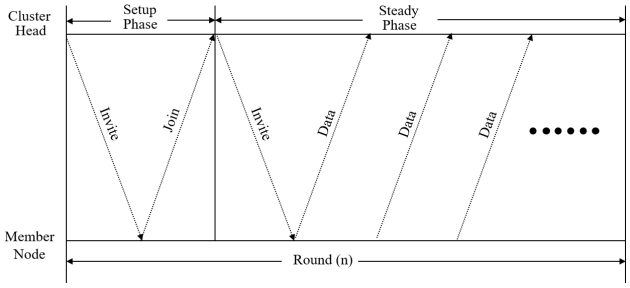

Fig. 2. TDMA scheduling mechanism based on clustering.

The network periodically reinitializes to select new CHs, addressing the rapid energy depletion of CHs due to their data collection and forwarding duties. The primary challenge is to select CHs to enhance network longevity optimally. The DACHER protocol integrates various chain-based clustering methods to extend the network's lifespan and scalability. The key features of clustering methods are summarized in Table I, highlighting the advantages and operational mechanics of optimizing energy efficiency and network performance.

The proposed protocol offers the following advantages. First, it utilizes a chain topology structure to minimize intercluster transmission distance. Strategically plan cluster distribution to avoid voids near the BS. By rationally dividing the area, clusters can be distributed regularly and evenly, ensuring optimal network performance. Implement PR to prevent single points of failure. Second, PR should be implemented to avoid single points of failure. Introduce rules to differentiate clusters in hot spots and non-hot-spot regions, ensuring the accuracy and quality of clusters for enhanced network stability. By rationally dividing the area, clusters can be distributed regularly and evenly. Third, select CHs based on remaining energy, density, location, and distribution, establishing a relationship between the number of nodes, cluster distribution, and cluster quality. This approach helps reduce energy consumption and extend network lifetime. Besides, this is suitable for large-scale networks with good stability and scalability.

B. Clustering Protocols

Table II provides a comprehensive classification and analysis of the technical characteristics of hierarchical routing protocols, highlighting the unique features and advantages of DACHER within the context of existing routing methodologies.

The traditional clustering protocol considers the classical factor and uses the basic method to select CHs and form clusters. Early clustering protocols have certain limitations as they only minimize the overhead by randomly selecting CHs [13]. To address these limitations, Pachlor and Shrimankar [14] proposed an LAR-CH protocol. This method uses the k-means++ algorithm for clustering nodes, which helps reduce the risk of premature node death to some extent. Also related, Chen et al. [15] propose WLEACH-CK, a weighted k-means-based algorithm to efficiently cluster sensor nodes in

TABLE I
MAIN FEATURES OF EXISTING ROUTING METHODS

Clustering Method	Advantages	Disadvantages
Partition-based clustering	Simple and efficient for large data. Low time complexity. Low space complexity.	Local optimization. Sensitive to noise and outliers. Only for numerical data.
Hierarchical clustering	Good interpretability. High quality clustering.	High computational complexity. High costs when applied to large-scale and high-density networks.
Density-based clustering	Insensitive to noise. Can find clusters of arbitrary shapes.	The results of clustering are closely related to the parameters. Inefficient in dense networks.
Grid-based clustering	Dependent on the number of input data. Low processing time. High performance with irregular data distributions.	The efficiency of this algorithm is improved at the cost of accuracy. Parameter sensitive. Unable to deal with dimension disaster.
Model-based clustering	The classification of "cluster" is not so "hard", but in the form of probability. The characteristics of each cluster can also be expressed by parameters.	When the number of distributions is large and the amount of data is small, its execution efficiency is not high.
Fuzzy-based clustering	The algorithm has good clustering effect for data satisfying normal distribution. The algorithm is sensitive to outliers. High performance with split clusters.	FCM cannot be guaranteed to converge to an optimal solution. The algorithm's performance depends on the initial cluster center.

WSNs. It selects the node with the smallest weighted distance as the CH to achieve a load balance. Nevertheless, these approaches fail to mitigate the transmission inefficiency of distant orphan nodes and the potential for CH overload.

Considering the nonuniform distribution of LEACH CHs, Al-Zubi et al. [16] introduce the load-balancing CH (LBCH) protocol designed to enhance the energy efficiency and lifetime of WSNs. LBCH focuses on minimizing energy consumption and distributing the workload evenly across all network nodes. Moussa et al. [17] focused on addressing frequent reclustering and topology changes in WSNs with the energy-efficient CH rotation protocol (ECRP). This algorithm manages CHs and relay faults by filtering CHs based on nodes' residual energy and a threshold function. Simultaneously, selecting CH nodes may require long-distance data transmission, which increases energy consumption. Therefore, it is essential to consider distance factors in the CH selection process to optimize energy efficiency.

Rawat and Chauhan [18] present a novel cluster-based routing protocol for WSNs called heterogeneous network-based clustering (HNBC). The goal of HNBC is to address the issues of energy consumption and network lifetime, which are critical for the performance of WSNs. Micheletti et al. [19] introduced the CER-CH algorithm, which combines a top–down defined routing tree with a rotation mechanism. This approach balances energy consumption among nodes by integrating a new rotation heuristic algorithm with a top–down routing tree definition. Additionally, Kaur et al. [20] designed a heterogeneous load-balancing clustering (HLBC) method. This method divides the network into regions and deploys more efficient nodes near the BS to manage network load, thereby avoiding grid holes near the BS and improving network connectivity. Overall, these improved strategies optimize the selection and load management of CHs through various methods. However, due to the involvement of multiple factors in the CH selection process, traditional deterministic algorithms often face challenges in achieving optimal clustering solutions.

Fuzzy logic is mainly used to address the uncertainties inherent in the clustering process [21]. By considering multiple factors simultaneously, this method enables more intelligent decision-making, improving network stability and energy efficiency. Numerous studies have leveraged fuzzy logic techniques for clustering applications. Regarding the selection of CHs, Murugaanandam and Ganapathy [22] introduced a novel method named "reliability-based enhanced technique for the ordering of preference by similarity ideal solution (RE-TOPSIS)" integrated with fuzzy logic for improving the selection of CHs in WSNs. The goal is to extend the network lifetime by making the CH selection process more efficient and reliable. Naik and Shetty [23] proposed a hybrid layered protocol, I-FLAG, which improves network stability. Unlike previous methods that used a single approach for CH selection, I-FLAG divides the CH election into two stages: CH election and secondary cluster head (SCH) election. The CH election stage is implemented through a game theory protocol, while the SCH election stage uses a fuzzy inference system. Hou et al. [21] presented an energy-efficient clustering routing (EFCR) protocol based on fuzzy inference. This protocol designs two types of clustering (clustering type1 and clustering type2) and alternates between them in different rounds based on thresholds to reduce energy consumption caused by unsuitable nodes being continuously selected as CHs, thereby extending the lifespan of the WSN.

Additionally, Baradaran and Navi [24] proposed a clustering algorithm focused on generating high-quality clusters (HQCA-WSN) to reduce errors within and between clusters. This algorithm uses the residual energy, maximum and minimum distances, and the maximum and minimum energies within the cluster as inputs to the fuzzy system. Ali et al. [25] developed a CH selection method based on the Enhanced Fuzzy Logic Zone Stable Election Protocol for Cluster-Head Election (E-FLZSEPFCH) for multipath routing in WSNs. This method optimizes energy consumption and improves

TABLE II
ORGANIZATION OF RELEVANT LITERATURE

Protocol Name	Features	Protocol Type	CH Selection
LAR-CH	Based on the K-Means++ algorithm, re-cluster for each round.	Partition-based	Based on a dynamic threshold.
WLEACH-CK	Based on weighted K-means select the node with the smallest weighted distance as the CH.	Partition-based	Based on the smallest weighted distance.
MSCD	Adds head-node rotation + backup head nodes for fault-tolerance and balanced workload.	Model-based	Backup heads are chosen by the highest energy-to-distance ratio, and main/backup roles rotate periodically for load balancing.
UCRTD	Introduces a distance and energy weighted multihop relay scheme that prolongs network lifetime.	Model-based	Waiting-time optimisation plus the energy-weighted relay rule pick the final CHs for robust load balancing.
EEHCHR	Hybrid clustering with fuzzy C-Means and emphasizes reducing the overhead.	Model-based	Depends on an adaptive fitness function incorporating residual energy and Euclidean distance.
EOCGS	Introduces an optimum number of cluster heads and grid heads; employs grid-based clustering to reduce excessive energy usage.	Model-based	Uses a fitness function based on residual energy, location, and distance to determine both CHs andgrid heads.
CER-CH	Combines a top-down routing tree with a rotation mechanism for balanced energy consumption.	Partition-based	Integrates a new rotation heuristic algorithm with a top-down routing tree definition.
MRCH	Builds on RCH-LEACH; integrates residual energy and distance factors to optimize cluster-head election.	Partition-based	Adopts an enhanced LEACH approach. CH is chosen via thresholds on energy and location for more robust load balancing.
EFCR	Energy-efficient clustering routing protocol, alternates clustering types based on thresholds.	Fuzzy	Reduces energy consumption by avoiding unsuitable nodes being continuously selected.
RE-TOPSIS	Uses fuzzy logic to improve CH selection, extending network lifetime.	Fuzzy	Makes CH selection process more efficient and reliable.
HQCA-WSN	Focuses on generating high-quality clusters.	Fuzzy	Uses residual energy, maximum/minimum distances, and maximum/minimum energy within the cluster.
I-FLAG	Hybrid layered protocol, improves network stability.	Heuristic	Uses game theory for CH election and fuzzy inference for SCH election.
LBR-GWO	Construct a CH selection mechanism with maximum efficiency.	Heuristic	Based on the selection mechanism with maximum efficiency.
E-GLBR	Improves CH selection and enhances energy efficiency in IoT-enabled WSNs.	Heuristic	Aims to optimize energy consumption, stability, and overall network performance.
GWOA-CH	Dual-CH layered routing protocol combining GWO and WOA with a time-interval CH re-election mechanism.	Heuristic	Reduces energy consumption and addresses premature energy depletion in WSNs.
DACHER	Chain-based for data communication regular division of CH, period rotation.	Model-based	Based on residual energy, density, position and division of WSNs.

network reliability and lifespan by utilizing dynamic, uneven cluster ranges and making multiparameter fuzzy logic decisions based on energy, distance, and queue length.

In WSNs, the clustering problem is generally considered an NP-hard problem [26], [27]. To address this challenge, numerous researchers have proposed various solutions. Typically, heuristic clustering protocols provide optimized solutions for different clustering issues, improving the network's lifespan and performance. For instance, John and Rodrigues [28] proposed a clustering protocol based on Taylor series and crow search algorithm (CSA). The optimal selection of CHs uses memory of previous positions or information from earlier iterations to update new CHs.

Similarly, Dwivedi et al. [29] propose a GWO algorithm (LBR-GWO), which develops a hierarchical routing algorithm for WSNs. This algorithm layers the area and constructs a CH selection mechanism with maximum efficiency, effectively improving the network's ability to run further iterative communication operations under limited interference and fading effects. In addition, Liu et al. [30] innovatively proposed a dual-CH layered routing grey wolf and whale optimization algorithm-based cluster-head election protocol (GWOA-CH) based on a hybrid swarm intelligence optimization algorithm. By combining the GWO and whale optimization algorithm (WOA), and introducing a time-interval-based CH re-election mechanism, this protocol reduces the energy consumption caused by frequent cluster formation and effectively addresses the issue of premature energy depletion in specific advantageous nodes within WSNs. These heuristic-based protocols significantly improve clustering efficiency and network performance by offering sophisticated solutions to the complex clustering problem in WSNs.

Recent work has also focused on devising refined approaches to ensure efficient cluster formation and load distribution in large-scale WSNs. For instance, Panchal and Singh [31] proposed an energy-efficient hybrid clustering and hierarchical routing (EEHCHR) protocol, which leverages fuzzy c-means (FCM) to cluster nodes adaptively and integrates a hierarchical packet routing scheme to reduce excessive consumption of CHs. They further extended their strategy with a modified RCH-LEACH (MRCH) approach [32], enhancing traditional LEACH by adding residual energy and distance

factors to manage CH selections, thereby reducing overhead and prolonging network lifetime in dense WSN deployments. Meanwhile, an energy-efficient optimum number of CH and grid head selection (EOCGS) algorithm [33] introduces grid heads for better balancing intercluster routing in multihop transmissions. Despite these advances, most existing schemes remain reactive and locally scoped, allowing energy hot spots to emerge before countermeasures are triggered.

The key advantage of DACHER lies in its proactive, network-wide load equalization. Instead of waiting for an event, DACHER periodically sweeps sector boundaries through neighboring rings and re-elects CHs and relay nodes before any energy hot spot can form. This pre-emptive rotation prevents early battery depletion along critical relay paths, distributes workload uniformly, and ultimately extends the network's operational lifespan—an outcome that MSCD's local, event-driven mechanism cannot achieve independently.

Previous studies have achieved significant results in energy efficiency, load balancing, and network lifetime extension through the use of protocols such as LEACH, CER-CH, and ECRP, as well as fuzzy logic, heuristic algorithms (e.g., RE-TOPSIS, I-FLAG, and high-quality clustering algorithm (HQCA)-WSN), and various intelligent optimization algorithms (e.g., E-GLBR, GWOA-CH, and MRCH). However, there remain limitations in optimizing intracluster and intercluster distances, which require further exploration by integrating the advantages of different algorithms to develop more efficient solutions. Therefore, this article proposes DACHER, which is aimed at optimizing energy consumption, extending network lifespan, enhancing sustainability, and improving cluster quality to enhance the performance of WSNs comprehensively.

III. Background: System Modeling

In this section, we detail the system model used in DACHER. The network and energy-consumption models are presented in Sections III-A and III-B. Fig. 3 shows the overall technological process of our proposed method.

A. Network Model

Building on the work described in Section II, this article proposes a novel dynamic region-based protocol, DACHER. The network model used in this study is composed of a ring structure, in which sensor nodes are randomly distributed in a circular sensing area centered on a BS. In this WSN model, these sensor nodes continuously detect the region during the network operation until the energy is exhausted. The network is divided into concentric rings, each ring's width proportional to its distance from the BS. Let r_0 be the initial radius of the first ring, and let ω govern ring growth. For layer i, we define: $R_{i-0} = \omega^{i/2} * r_0$ and $R_i = R_{i-0} - R_{(i-1)-0}$, so that the sensing field is divided into h layers $\{R_1, R_2, \ldots, R_h\}$. This ensures a scalable partitioning of the field, allowing each ring to have an appropriate width as the network size increases.

On this basis, the following assumptions are made about the WSNs.

1) There is a single BS in the network.
2) The sensor nodes are randomly distributed, and all nodes are fixed at a static location.
3) Each sensor node contains the same amount of energy, which decreases with transmitting information (sending and receiving messages).
4) Each sensor node can monitor, aggregate, transmit, and receive data from other sensor nodes or BS.

Fig. 4(a) shows a process schematic of the CHs that collect information from the respective cluster and send it to the BS. The WSN scenario adopted is a very common, with a single BS, homogeneous sensor nodes randomly distributed and fixed [34].

The assumptions of our scheme are reasonable for a real typical scenario. For example, multiple nodes share the same BS. The BS utilizes an energy collection method to provide energy, thus providing a continuous energy supply. Each node contains the location information via GPS and a location algorithm [35]. It can also estimate the energy level due to the energy model of specific hardware. In addition, the nodes have the ability to forward data and transmit in a multihop manner, acting as CH. The nomenclature shows all the definitions of variables that are employed throughout this article.

B. Energy-Consumption Model

The energy consumption of sensor nodes mainly comes from three aspects: the sensing energy consumption of the sensor module (also known as sensing energy consumption), the control and data processing energy consumption of the processing module, as well as the wireless communication energy consumption of the transceiver module and respective antenna. Therefore, when designing low-power WSN protocols, we should reasonably control the state of wireless communication and comprehensively consider factors such as packet length, communication distance, and transmission power. In this article, DACHER adopts the first-order radio model based on the free-space model and multipath fading channel to maximize energy utilization and achieve a WSN with good scalability, less collision probability, and low energy consumption.

As shown in Fig. 4(b), when a node sends data, the transmitter sends data back and utilizes an amplification circuit to augment the signal (this consumes energy). When a receiver gets data, it uses a receiving circuit to parse it, so that only the energy of the received signal is consumed at the receiving end.

During the data communication between nodes, the energy consumption of the nodes is a function of the distance between the transmitter and the receiver. The free-space model is used for short distances (d^2 power loss), while the multipath fading model is employed for long distances (d^4 power loss). When the node X sends a k-bit message to the node Y, the energy consumed by the radio can be calculated as follows:

$$E_{\mathrm{Tx}}(k,d) = \begin{cases} kE_{\mathrm{elec}} + k\varepsilon_{\mathrm{fs}}d^2, & d \le d_0 \\ kE_{\mathrm{elec}} + k\varepsilon_{\mathrm{mp}}d^4, & d > d_0 \end{cases} \tag{1}$$

where E_{elec} is the energy consumed per 1-bit data transmission by the transmitter or receiver circuit, d denotes the distance

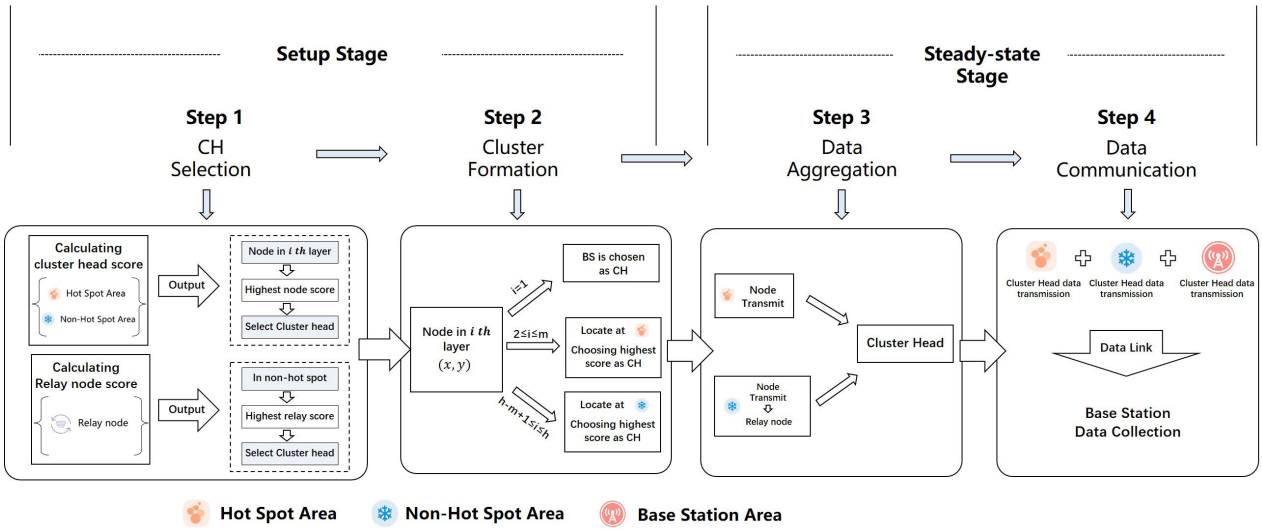

Fig. 3. Illustration of technological workflow.

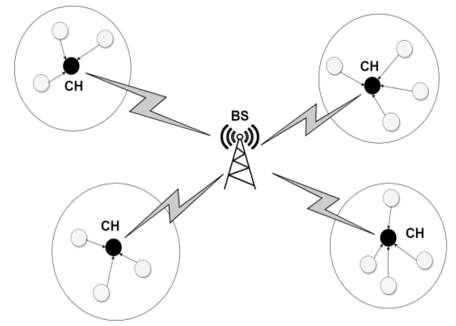

(a)

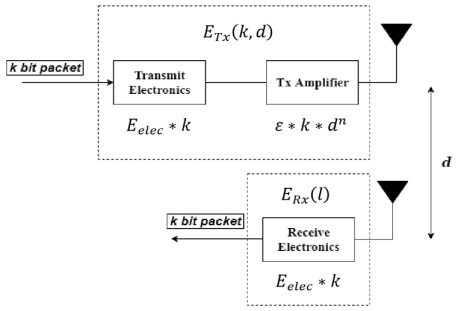

(b)

Fig. 4. Network model and energy consumption. (a) Representation of the network configuration. (b) First-order energy model for radio transmission.

between the sending node (node X) and the receiving node (node Y), and d_0 is utilized the threshold of the transmission distance ($d_0 = (\varepsilon_{\mathrm{fs}}/\varepsilon_{\mathrm{mp}})^{1/2}$). $\varepsilon_{\mathrm{fs}}$ and $\varepsilon_{\mathrm{mp}}$ are the energy loss coefficients of the power amplification circuit under different channel propagation models, where the selection of the channel mode is affected by the transmission distance. While with $d < d_0$, the free-space model is adopted, and the energy loss coefficient of the power amplification circuit is $\varepsilon_{\mathrm{fs}}$. Otherwise, the multipath fading channel model is employed, so the energy coefficient is $\varepsilon_{\mathrm{mp}}$. The calculation of the energy consumed for receiving k bits data can be seen in the following equation:

$$E_{\mathrm{Rx}} = kE_{\mathrm{elec}}. \tag{2}$$

IV. DACHER Algorithm

The proposed DACHER protocol operates on the network layer of the hierarchical model of WSNs, which is similar in structure to the open system interconnection (OSI) network model.

Three consecutive operations are contained in this protocol: cluster operations (clustering), region iteration, and network operations. These operations include the following.

1) Clusters are generated by the ring structure of the network to average the CH selection range of competition.
2) The procedure of CH selection is accomplished by using the objective function at the active nodes in each specific region. Meanwhile, PR is used for region iteration to adjust the competitive range of CH selection dynamically.
3) The data transfer phase is performed.

Once the node is deployed, CH sends and receives control packets to obtain information about other nodes, such as IDs, coordinates, and energy values. Each sensor node calculates and updates its distance to the adjacent nodes and the CHs by utilizing the coordinates of the nodes. These Euclidean distances and energy values are specifically used to optimize network topology and achieve the optimal path for packet transmission.

Remark: "The clustering process balances energy consumption across nodes by selecting CHs with optimal energy and location factors. This approach helps extend the network lifetime by ensuring CHs do not deplete energy prematurely."

Since clustering is an optimization problem, it is paramount to select CH dynamically. Also, each network operation must choose the most appropriate CH configuration to ensure energy balance across the network topology. The remaining energy and position of nodes will be calculated at the end of each

round. Then, the next round of CH allocation is determined based on this calculation result. This cycle will continuously repeat until all sensor nodes die. The detailed description of the above process is shown in Algorithm 1. In addition, the communication procedure is presented in Algorithm 2. Further discussion of both algorithms can be found from Sections IV-A–IV-C.

A. Cluster Operation

The clustering operation in this article is divided into two stages: data setting and data transmission. The setup state includes cluster partition and CH selection. In this state, nodes are divided into clusters by the appropriate division. Then, the value of the objective function is calculated for the active nodes in the network. The node with the highest score will be qualified as CH, and the remaining will be referred to as member MNs.

The setup state follows the data transmission, subdivided into the data aggregation and transmission phases. In this stage, the CH assigns a TDMA schedule to MNs in the cluster, which can schedule MNs to transmit data. Next, all the information about the CH and TDMA scheduling packets will be broadcast to the whole cluster. Based on the time interval of TDMA scheduling packets, each node sends sensory data to the respective CHs in the cluster. In the above process, the CH consumes energy faster than the MNs. Therefore, it is necessary to perform reclustering at certain time intervals to change the role of CH, which can balance energy consumption.

In this article, a reclustering process is performed by PR. Following each rotation, a new topology is formed to preserve uniform coverage and enhance energy efficiency in the WSN. The rotation interval is determined by the combined duration of cluster formation and the stable data transmission phase. Moreover, because each round's length is dynamically adjusted according to the number of active nodes, the optimal interval must be carefully balanced: if it is set too long, some CHs may drain their energy prematurely and compromise network coverage; if it is too short, frequent reclustering leads to additional control overhead and unnecessary resource consumption. In our design and experiments, we account for these tradeoffs, ensuring that the reclustering cost is appropriately included in the overall energy budget while avoiding the pitfalls of excessively long rotation intervals.

In the initial stage of the network, the BS divides the monitoring area into Z ($Z = 4$) sectors uniformly. Then, the BS stratifies the monitoring area as the center according to different radiation ranges. Alternatively, the BS is directly regarded as the CH in the first ring. Nodes near the BS consume less energy during transmission, while nodes in the edge area far from the BS consume more energy. Therefore, the monitoring area is divided into hot spots and non-hot-spot areas by the distance to the BS. Each annular ring in DACHER covers a specific radial distance from the BS. By subdividing each ring into angular sectors, we effectively cap how many nodes are in each region. Hence, within each sector, only a subset of nodes competes to become the CH, inherently limiting the total number of CHs across the entire network.

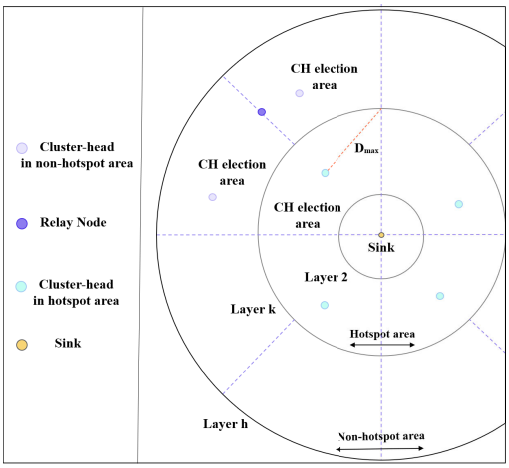

Fig. 5. Initial division of areas.

As shown in Fig. 5, the hot-spot area is set as the ring from 2 to k, and the range of the non-hot-spot region is from $(h - k + 1)$ to h. This division is shown in lines 2–6 of Algorithm 1.

Remark: "To enhance efficiency further, we design separate objective functions for the hot-spot and non-hot-spot rings. Specifically, density factors are prominent in the hot-spot area since nodes closer to the BS tend to be more numerous and handle heavier intracluster load. Meanwhile, the non-hot-spot objective considers location and residual energy as primary determinants, acknowledging that nodes in peripheral rings suffer from greater path loss and require additional relay support. By customizing the CH selection criteria for each region, DACHER better adapts to varying node densities and transmission distances, in contrast to uniform or single-threshold-based approaches often seen in conventional clustering protocols."

1) Hot-Spot Area: As illustrated in Fig. 5, the network is partitioned into two primary zones according to their proximity to the BS. The hot-spot area encompasses the annular layers from layer 2 through layer k. Within this annulus, the sectors delimited by concentric circles and radial lines constitute the CH election areas. After the cluster partition, selecting an appropriate CH in each electoral district becomes crucial.

To reduce communication consumption between nodes, the node adjacent to the center line of the election region is more likely to be chosen as the CH. However, considering only the location factor while ignoring the residual energy of the selected CH can easily lead to the premature failure of the CH with low energy. In addition, DACHER takes the density factor into account. If the number of neighbor nodes of the CH is relatively small, it will also lead to excessive energy consumption.

Therefore, DACHER selects location, residual energy, and density as candidate parameters for selecting CH in hot-spot regions. The scoring function of CH selection can be described as follows:

$$\mathrm{CH}(j)_{\mathrm{score}} = C_1 \frac{D_{\max} - D_j}{D_{\max}} + C_2 \frac{E_j}{E_0} + C_3 \rho \qquad (3)$$

where $\mathrm{CH}(j)_{\mathrm{score}}$ denotes the fraction of node j. C_1, C_2, and C_3 are the weighting factors that satisfy the condition $C_1 + C_2 + C_3 = 1$. This constraint ensures that the contributions of the position factor, residual energy, and node density are normalized and can be directly interpreted as their relative importance: a higher C_1 places more emphasis on selecting nodes closer to the centerline (thus reducing intracluster transmission distance), while a higher C_2 favors nodes with more residual energy to extend network lifetime, and a higher C_3 rewards nodes with greater local density, thereby ensuring robust connectivity. In our experiments, the typical settings are $(C_1, C_2, C_3) = (0.3, 0.4, 0.3)$ or $(0.2, 0.5, 0.3)$, which were determined through extensive tuning to achieve a balanced energy consumption and optimal network performance. $D_{\max}$ denotes half of the chord length subtended by the outer boundary arc of the CH electoral area, in which node j resides. D_j is the vertical distance from the node j to the centerline of the election area, E_j is the remaining energy of the node j, and E_0 is the initial energy.

ρ is defined as the density factor, which is used to measure the number of other nodes near the node j. In the actual monitoring scenario of WSN, the nodes are randomly scattered in the monitoring area. Therefore, the number of adjacent nodes should be considered during CH selection. If the node has few or no neighbors, the node is not suitable for a CH. Here, adjacent nodes are defined as nodes within the maximum coverage communication range R. Density ρ can be calculated by using the following equation:

$$\rho = \frac{j \cdot N_{\mathrm{nb}}}{N} \tag{4}$$

where N represents the number of nodes in the area where the node j is located. N_{nb} represents the number of neighboring nodes of the node j within its standard communication radius, which can be calculated using the following equation:

$$j \cdot N_{nb} = \{i \vee d(i, j) \leq R, i \in n\}, j \in \{1, 2, \ldots, n\} \tag{5}$$

where the node i refers to the other node in the region, and n is the number of nodes within the monitoring range of the node j, that is, the number of nodes i. Moreover, R is the maximum communication range, defined as half of the width of the ring where the node j is located in this article.

The CH selection procedure in the hot-spot area is presented in lines 4 and 5 of Algorithm 1.

2) Non-Hot-Spot Area: As shown in Fig. 5, the non-hot-spot area is predefined from $(h - k + 1)$ to h in this article. Since the non-hot-spot area is far from the BS, the nodes will inevitably consume more energy during transmission. As depicted in Fig. 6(a), as the number of layers increases, the area responsible for the CH will gradually increase, and the amount of data received increases similarly, eventually leading to the premature death of the peripheral nodes. Therefore, we equally divide each sector into two small sectors with $\alpha = 45°$ in the non-hot-spot area: two CH election areas. The CH election area of the non-hot-spot area is bounded by the adjacent layers' concentric circles, sector radius lines, and centerlines.

Nodes must transmit over longer distances in non-hot-spot rings far from the BS. Suppose direct CH-to-BS transmission is employed in these regions. In that case, it often leads to the formation of hot spots near the BS or causes premature energy depletion of CHs located farther from the BS. By introducing relay nodes roughly at the middle of each ring segment, DACHER adds an intermediate hop, ensuring that no single

Algorithm 1 Cluster Establishment Phase

1: **Input:**
The number of layers h; node-layer index i; outermost hot-spot layer m; radius of the first layer R_0; rotation angle β; node coordinates (x_i, y_i)
Initial energy E_0; cluster-head CH_{all}; relay-node RE_{all};
2: **Output:**
The fraction of node $j\mathrm{CH}(j)_{\mathrm{score}}$, candidate CH $CH(j)_{\mathrm{score}}$ and relay nodes $R(K)_{\mathrm{score}}$
3: **Begin**
4: **for** $0 < \beta \leq \pi/2$ **do**
if $i = 1$ **then**
The BS is chosen as the CH
elseif $2 \leq i \leq m$ **then**
Calculate node scores with (3)
elseif $(h - m + 1) \leq i \leq h$ **then**
for $K \leftarrow$ *nodes in each non-hot election zone* **do**
Calculate node scores with (7)
end for
for $j \leftarrow$ *nodes in each non-hot election zone* **do**
Calculate node scores with (6)
end for
end if
Update CH_{all} and RE_{all}
end for
Return CH_{all}, RE_{all}

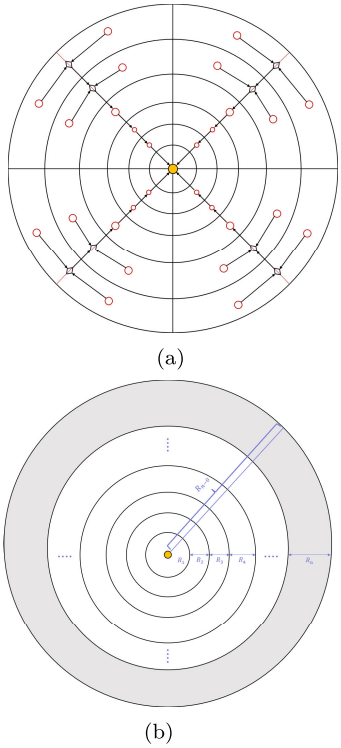

(a)

(b)

Fig. 6. Data transfer process and hierarchical model of DACHER. (a) CH transmission. (b) Hierarchical network model.

CH is forced to handle large distances independently. Thus, CHs selected on both sides of the centerline can relieve the burden of receiving and fusing data by a single CH. Moreover, to reduce the energy loss transmitted to the BS, DACHER introduces a relay node to receive the data collected by the CHs on both sides.

Next, the relay node aggregates and forwards the data to the next layer. Finally, a chained communication link shown in Fig. 6(a) is established to transmit the packets to the BS layer by layer in the transmission phase. With the addition of relay nodes, selecting suitable CHs can significantly affect the network's lifetime. The residual energy determines the amount of data the CH receives, an essential factor in selecting the CH. The CH selection procedure in a non-hot-spot area is presented in lines 10 and 11 of Algorithm 1.

Further performed in the experimental section, this article conducts a series of relative tradeoffs to evaluate the influence of various parameters on energy loss through many experiments. In addition, the transmission energy consumption within the cluster would be reduced while the CH is close to the center of the selection area. Here, CH selection in the non-hot-spot area only considers location and residual energy. Then, the standard scoring function of the candidate CH is as follows:

$$\mathrm{CH}(j)_{\mathrm{score}} = (1-\theta)\frac{E_j}{E_0} + \theta\left[-\left(\frac{D_{\max}-D_j}{D_{\max}}-1\right)^2\right] \tag{6}$$

where θ is a weight adjustment factor (ranging from 0 to 1) that allows us to fine-tune the relative importance between the residual energy and the node's position. The θ value closer to 0 emphasizes energy, while a value closer to 1 emphasizes the positional factor, with default values such as $\theta = 0.5$. E_j indicates the residual energy of the node j in the region, and E_0 indicates the initial energy. D_j is the vertical distance from the node j to the centerline, and $D_{\max}$ represents the same value as in (3).

To establish a chain communication link from outside to inside, a relay node is elected near the centerline of each layer in the non-hot-spot area. In this study, the purpose of introducing relay nodes is to construct the optimal path and reduce the burden of CHs, so we only consider the two factors of location and remaining energy. The standard scoring function of relay nodes can be expressed as follows:

$$R(K)_{\mathrm{score}} = \varphi\frac{E_k}{E_0} + (1-\varphi)\frac{D_{\max}-D_k}{D_{\max}} \tag{7}$$

where φ (also in the range [0, 1]) adjusts the tradeoff between the node's residual energy and its position relative to the centerline for relay node election, with default values such as $\varphi = 0.4$. The node K is a node other than CHs in the area enclosed by concentric circles and sector radius lines of adjacent layers. E_0 represents the initial energy, and E_k denotes the remaining energy. D_k is the vertical distance from the node K to the centerline, and $D_{\max}$ represents the same value as in (3).

In summary, our scoring functions [see (3), (6), and (7)] integrate location, residual energy, and density for hot spots, or the combination of location and residual energy for non-hot spots. By recalculating these scores in each round and restricting the competition to a constrained sector, we "automatically" keep the number of CHs balanced. Higher energy nodes near ideal positions, thus, have a greater chance of election, reducing suboptimal CH allocations.

The selection process of relay nodes in a hot-spot area is presented in lines 7 and 8 of Algorithm 1.

3) Data Transmission: As shown in Fig. 6(a), CHs are selected near the centerline (approximately at the exact location in each layer) in the hot-spot area, and CHs are located on both sides of the centerline in the non-hot spot.

Relay nodes are located near the centerline in the non-hot-spot area. Therefore, CHs in the hot-spot area and relay nodes in the non-hot-spot area can establish a chain communication link from outside to inside to transmit packets collected from each cluster to the BS. The data transmission process is shown in Algorithm 2.

Remark: "The chain communication structure from outer to inner layers minimizes long-distance transmissions, thereby saving energy and reducing network congestion, which improves overall efficiency and data reliability."

B. Regional Iteration

In this section, we discuss the iteration present in a DACHER region.

1) Hierarchical Model: Considering that the nodes close to the BS must undertake more forwarding tasks, DACHER adopts a circular layered interval that gradually increases from the inside to the outside, which can adjust the competition range of CH selection in each layer, as depicted in Fig. 6(b). The layering is calculated by the following equation:

$$\begin{cases} R_1 = r_0, \quad i = 1, \\ R_{i-0} = \omega^{i/2} * r_0, \quad i \geq 2, \\ R_i = \omega^{i/2} * r_0 - \omega^{(i-1)/2} * r_0, \quad i \geq 2 \end{cases} \tag{8}$$

where R_1 denotes the radius of the first layer of the network, R_{i-0} represents the distance from the ith layer to the BS, R_i presents the width of the circular region of the ith layer, r_0 denotes the initial radius of the first layer, and ω denotes the radius factor, which is set to 2 in this article.

Remark: "The hierarchical model optimizes CH selection, reducing reclustering frequency and enhancing scalability for larger networks."

2) Regional Rotation: To balance the energy consumption of nodes and reduce the possibility of a single node being repeatedly selected as the CH, the division area is not fixed. DACHER will continuously change the CH in each area by systematic rotation. The process of regional rotation is presented in Algorithm 1.

As shown in Fig. 7, all centerlines and radius lines rotate counterclockwise simultaneously. β represents the counterclockwise rotation angle after a predefined number of rounds of data collection. We now formally express the rotation of annular sectors through the angle β. Let $\theta_{\mathrm{Election}}(n)$ be the initial boundary angles for sector n. After p rotation intervals, the sector boundary rotates counterclockwise by $p \cdot \beta$. Specifically, let the initial angular boundaries of sector n be $\theta_{\mathrm{Election}}(n) = [2\pi(n-1)/z, 2\pi n/z]$, where z is the total number of sectors. After p rotation intervals, these boundaries become $\theta_{\mathrm{Election}}(n) = [2\pi(n-1)/z + p\beta, 2\pi n/z + p\beta]$.

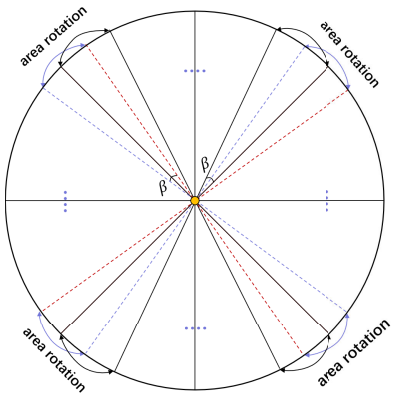

Fig. 7. Rotation of CH selection areas ($\beta = 13°$).

This rotation guarantees that no single node remains fixed in the same sector indefinitely, thus balancing the energy load among all nodes in the network over time. After the rotation, each node can identify its region by the rotation angles, so the energy consumption generated by reclustering is nonadditional.

In addition, long time intervals will excessively consume the energy of CHs, while short time intervals lead to frequent clustering, resulting in additional overhead. Thus, it is essential to consider the time interval for reclustering. We specify that the coordinates of nodes in the network are not changed with rotation. The angle of the centerline of the nth region, the range of the angle of the nth CH-selected region (distinguishing between hot-spot and non-hot-spot areas), and the location of the nth CH-selected region after P-round rotation (distinguishing between hot and non-hot-spot areas) can be calculated separately using (9)–(11). The detailed procedure for regional rotation is outlined in Algorithm 1.

Remark: "In WSNs, clustering remains a cornerstone for efficient topology management. Unlike previous dynamic clustering methods that primarily rely on random or probabilistic CH elections or static subdivisions, DACHER adopts an annular RB deployment. Each ring is further subdivided into angular sectors, and we periodically rotate these boundaries to ensure that potential CHs do not remain in edge regions continuously. Through this lightweight rotation mechanism, no single node becomes a perpetual CH, and the ring sectors maintain balanced coverage across the entire sensing field. This approach effectively reduces the overhead of reclustering compared to centralized recalculations and combats 'hot spots' near ring boundaries"

$$\theta_{\text{Middle}}(n) = \frac{2\pi n}{z} - \frac{\pi}{z}, z = 4, n \in (1, 2, \ldots, z) \tag{9}$$

$$\theta_{\text{Election}}(n) = \begin{cases} \left[\frac{2\pi n}{z} - \frac{2\pi}{z}, \frac{2\pi n}{z}\right] & [1] \\ \left[\frac{2\pi n}{2z} - \frac{2\pi}{2z}, \frac{2\pi n}{2z}\right] & [2] \end{cases}$$
$$\text{s.t. } [1] \in \text{hot-spot area}, [2] \in \text{non-hot-spot area} \tag{10}$$

$$\theta_{\text{Election}}(p) = \begin{cases} \left[\frac{2\pi n}{z} - \frac{2\pi}{z} + p\beta, \frac{2\pi n}{z} + p\beta\right] & [1] \\ \left[\frac{2\pi n}{2z} - \frac{2\pi}{2z} + p\beta, \frac{2\pi n}{2z} + p\beta\right] & [2] \end{cases}$$
$$\text{s.t. } p \in Z^+, [1] \in \text{hot-spot area}, [2] \in \text{non-hot-spot area}. \tag{11}$$

C. Energy Consumption

The algorithm divides the network operation into a setup and a steady-state phase. In each round, the energy consumption is calculated based on the tasks completed by each node.

1) Setup Stage: In the setup phase, the BS transmits and receives control data packets with all nodes to initiate intracluster and intercluster communication. The control packet K_{cp} contains a short message to wake up nodes, which requests IDs, position, and energy from all sensor nodes. Equation (2) shows that the energy consumption for receiving control packets from the BS is $E_{\text{Rx}}(K_{\text{cp}})$.

In (1), the energy consumption for all nodes to send control packets (containing about IDs, position, and energy) to the BS is $E_{\text{Tx}}(K_{\text{cp}}, d)$. The receiver receives control packets and makes certain decisions, such as deciding which nodes to consider as CHs and how to coordinate the communication process from the CH to the BS. Then, all nodes (whether CH or MNs) also receive their status information from the BS using energy $E_{\text{Rx}}(K_{\text{cp}})$. Specifically, the energy consumed by CHs to send TDMA schedules to their MNs is as follows:

$$E_{\text{Tx}(\text{ch}_i)}\left(K_{\text{cp}}, d_{i-\text{Mem}}\right) = \sum_{i=1}^{\text{ch}_i} * \begin{cases} K_{\text{cp}} * E_{\text{elec}} + K_{\text{cp}}\varepsilon_{fs} d_{i-\text{Mem}}^2, & d \le d_0 \\ K_{\text{cp}} * E_{\text{elec}} + K_{\text{cp}}\varepsilon_{\text{mp}} d_{i-\text{Mem}}^4, & d > d_0. \end{cases} \tag{12}$$

The energy consumed by all MNs to receive the TDMA schedule from the CH is calculated by (2). The process of the setup stage is shown in the initialization phase of Algorithm 1.

2) Steady-State Stage: In the steady state, according to the TDMA schedule received from the CH, MNs send sensing data to CHs in the form of packets. Each CH is always ready to receive the sensed data from its MNs in the same cluster. The CH aggregates and converts the received sensory data into a single data stream, and then transmits it to the BS for processing. The total energy dissipated by all MNs to transmit the sensed data to their CHs is calculated by

$$E_{\text{Rx}(m_i)}(K) = \sum_{i=1} m_i * kE_{\text{elec}} \tag{13}$$

where m_i denotes the MNs in the series $i = 1, 2, 3, \ldots, n-L$ in the hot-spot area, and m_i of the non-hot-spot area indicates the MN in the series $i = 1, 2, 3, \ldots, n-L-R$.

Furthermore, n, L, and R represent the total number of all sensor nodes, CHs, and the relay nodes, respectively. All CHs spend energy to aggregate the data sensed from their MNs and themselves, calculated as

$$E_{\text{DA}(m_i+1)}(K) = kE_{\text{DA}} * \left(\sum_{i=1} m_i + 1\right). \tag{14}$$

In the non-hot-spot area, the CH sends the aggregated data to the relay node, and the consuming energy is shown in (13).

The energy consumed by the relay node to aggregate data is shown in the following equation:

$$E_{\mathrm{DA(CH}_i+1)}(K) = kE_{\mathrm{DA}} * \left(\sum_{i=1} \mathrm{CH}_i + 1\right) \tag{15}$$

where i expresses the number of CHs in the non-hot-spot area. Finally, the relay node will establish a chain communication link with the CHs of the hot-spot area to send the aggregated data to the BS layer by layer from outside to inside. The energy consumption can be calculated by the following equation:

$$E_{Tx(\mathrm{Round}_i)}(K) = \begin{cases} \left(\begin{array}{c} \sum_{i=h-1}^{i=2} E_{DA(\mathrm{Round}_i)} \\ + \sum_{i=h}^{i=2}\left(K_{\mathrm{cp}} * E_{\mathrm{elec}} + K_{\mathrm{cp}}\varepsilon_{fs} d^2_{ch_i - ch_{i-1}}\right)\end{array}\right), & d \le d_0 \\ \left(\begin{array}{c} \sum_{i=h-1}^{i=2} E_{DA(\mathrm{Round}_i)} \\ + \sum_{i=h}^{i=2}\left(K_{\mathrm{cp}} * E_{\mathrm{elec}} + K_{\mathrm{cp}}\varepsilon_{mp} d^4_{ch_i - ch_{i-1}}\right)\end{array}\right), & d > d_0. \end{cases} \tag{16}$$

This communication procedure is shown in Algorithm 2. The relay node in the outermost layer (h) receives and aggregates the data collected by CHs, consuming $E_{\mathrm{DA(Round}_i)}$. After that, the aggregation result is transmitted to the relay node at the $(h-1)$th layer, which consumes $(K_{\mathrm{cp}} * E_{\mathrm{elec}} + K_{\mathrm{cp}}\varepsilon_{\mathrm{fs}} d^2_{\mathrm{ch}_i - \mathrm{ch}_{i-1}})/(K_{\mathrm{cp}} * E_{\mathrm{elec}} + K_{\mathrm{cp}}\varepsilon_{\mathrm{mp}} d^4_{\mathrm{ch}_i - \mathrm{ch}_{i-1}})$. Further, the relay node needs to aggregate the data received at the outermost layer and the data collected by CHs on both sides, and transmit it to the relay node at the next layer. By analogy, according to the chain communication link, the relay node/CH of the outer layer is transferred to the relay node/CH of the inner layer until it is transferred to the BS. Next, the relay node of the hth layer only needs to send the managed data, without aggregating it at the outer layer. Therefore, during data transmission, the number of aggregations is $(h-2)$, and the number of transmissions is $(h-1)$.

Algorithm 2 Network Communication Procedure

1: **Input:**
Cluster-head CH_{all}; relay-node RE_{all}; node coordinates (x_i, y_i)
2: **Output:**
Total energy consumption of the CH nodes $E_{\mathrm{CH}s}$, the member nodes E_{Mem}, and the relay nodes E_{REs}
3: **Begin**
4: **for** *CHs within hot spot area* **do**
CHs transfer packets from outside to inside via (17)
end for
for *CHs within non-hot spot area* **do**
CHs transmit packets to the RE via (18)
end for
for *member nodes in the whole area* **do**
Nodes transmit packets to their corresponding CH via (19)
end for
5: **Return**;
Number of dead nodes n, residual energy E_r

3) Total Energy Expenditure: The total energy consumed by all CHs can be calculated by the following equation:

$$\begin{aligned} E_{\mathrm{CHs}} = {} & 2 * E_{\mathrm{Rx}}\left(K_{\mathrm{cp}}\right) + E_{\mathrm{Tx}(ch_i)}\left(K_{\mathrm{cp}}, d_{i-Mem}\right) \\ & + E_{\mathrm{Rx}(m_i)}(K) \\ & + E_{\mathrm{DA}(m_i+1)}(K) + E_{\mathrm{Tx}(\mathrm{Round}_i=2,3,\ldots,m)}(K) \end{aligned} \tag{17}$$

where $2 * E_{\mathrm{Rx}}(K_{\mathrm{cp}})$ indicates the fact that the CH dissipates energy twice when it receives requests for ID, location, and energy value. The total energy consumed by all relay nodes can be calculated by the following equation:

$$\begin{aligned} E_{\mathrm{REs}} = {} & 2 * E_{\mathrm{Rx}}\left(K_{\mathrm{cp}}\right) \\ & + E_{0(\mathrm{CH}_i+1)}(K) + E_{\mathrm{Tx}(i=h-m+1,\ldots,h)}(K). \end{aligned} \tag{18}$$

Similarly, $2 * E_{\mathrm{Rx}}(K_{\mathrm{cp}})$ denotes the energy dissipated twice as the relay node receives requests for ID, location, and energy level. $E_{Tx(i=h-m+1,\ldots,h)}(K)$ denotes the energy consumed by relay nodes to deliver data layer by layer in the non-hot-spot area. The total energy consumed by all MNs can be calculated by the following equation:

$$\begin{aligned} E_{\mathrm{Mem}} = {} & 3 * E_{\mathrm{Rx}}\left(K_{\mathrm{cp}}\right) \\ & + E_{Tx}\left(K_{\mathrm{cp}}, d_{i-\mathrm{sink}}\right) + E_{Tx}\left(K_{\mathrm{cp}}, d_{i-ch}\right) \end{aligned} \tag{19}$$

where $3 * E_{\mathrm{Rx}}(K_{\mathrm{cp}})$ denotes the energy loss of each MN in receiving control packets and the additional energy loss in receiving the TDMA schedule from its CH. The total energy consumption can be expressed as follows:

$$E_{\mathrm{total}} = E_{\mathrm{CHs}} + E_{\mathrm{REs}} + E_{\mathrm{Mem}}. \tag{20}$$

This article also analyzes the computational complexity of DACHER to prove the advantages of this method. In selecting the maximum network lifetime, DACHER dynamically chooses the CHs according to the calculated objective function. Then, DACHER sets the corresponding transmission mode for different CHs in other locations. Here, we define the number of nodes in the hot-spot/non-hot-spot area as n_h/n_f, respectively. The number of rounds in the network is r. The hot-spot area is responsible for selecting suitable nodes as CHs, so the time complexity of the hot-spot area is $O(n_h r)$. In non-hot-spot area, the calculation of the relay node is added, so the time complexity of the non-hot-spot area is $O(n_f^2 r)$. Finally, we can get the total time complexity as follows:

$$O\left(n_h r + n_f^2 r\right). \tag{21}$$

V. Math Experimental Result and Analysis

This section provides a detailed account of the evaluation process, including the methodology, configuration, and comparative analysis of results, to thoroughly demonstrate the effectiveness and advantages of the DACHER protocol.

A. Methodology

The systematic simulation experiments were conducted on the MATLAB R2018b platform. The methodology is briefly outlined as follows.

First, the impact of the rotation angle β and the number of nodes on the network lifetime of the DACHER protocol is

TABLE III
PARAMETER SETTINGS FOR HOMOGENEOUS SCENARIOS

Experiment	Number of Sensors	Coordinates	Deployment Area (m^2)	Initial Energy (J)
Exp200	200	(0, 0)	120 x 120	0.5
Exp350	350	(0, 0)	120 x 120	0.5
Exp500	500	(0, 0)	120 x 120	0.5
Exp1000	1000	(0, 0)	200 x 200	0.5

analyzed. Here, the network lifetime is defined by the number of surviving nodes.

Second, the performance of four hierarchical routing protocols is evaluated from two perspectives: the distribution of surviving nodes and the remaining energy.

Finally, we compared DACHER's network lifetime and stability period with those of the four baseline protocols. All comparative experiments employed an identical parameter set from [36] to ensure fairness.

B. Configuration

This study developed a comprehensive simulation model to evaluate the performance of the proposed DACHER protocol, specifically focusing on network lifetime. The simulation scenarios utilized in this study are summarized in Table III. To maintain consistency with established benchmarks, the network density across the scenarios was set within the range of 0.014–0.035 nodes/m^2, following guidelines from the literature [18]. To demonstrate the generalizability of the DACHER protocol, various experimental configurations were implemented with different numbers of sensor nodes. These nodes were randomly deployed on an x–y grid with the origin at (0, 0), covering monitoring areas of either 120×120 or 200×200 m^2. Each scenario included a single BS, strategically positioned at the center of the deployment area, as detailed in Table III. This setup ensures a standardized environment for evaluating the protocol's effectiveness under varying conditions. The relevant parameters and protocols are detailed in Table IV.

C. Performance Metrics

The following metrics are used to evaluate the performance of the DACHER protocol.

1) Number of Active Nodes: It is the number of nodes that survived at a particular simulation time.

2) Energy Consumption: It is the numerical value of the energy utilized during communication between nodes.

3) Stability Period Length: It is the time range from the start of network operation until the first node death (FND).

4) Instability Period Length: It is the time span from the FND until the LND.

5) Lifetime: The network lifetime is defined as the duration from the start of network operation to LND, representing the execution period of the process. Alternatively, it can also be described as the combination of the SPL and the instability period length (IPL).

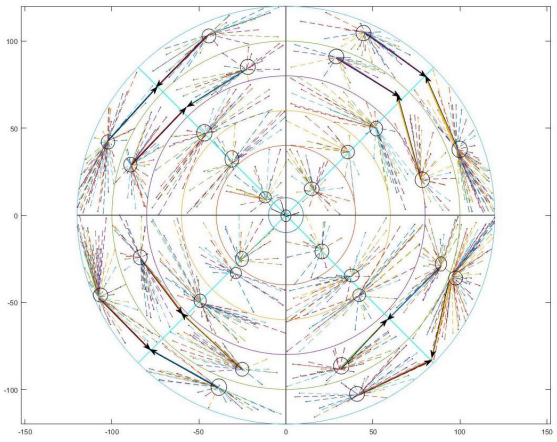

Fig. 8. Illustration of network communication.

D. Simulation Results and Analyses

1) Simulation Results: In this section, we present the simulation results in detail. First, Fig. 8 shows the simulation results with the parameter ($n = 350, I = 6, Z = 4$, and $\beta = 13°$). The entire ring is divided into four districts according to the coordinate axis, and each area comprises six rings. The first ring is not divided into different partitions, and the nodes in the first ring directly transmit the sensing data to the BS. The three inner rings from 2 to 4 are hot-spot areas, and the last two outer rings are non-hot-spot ones.

In Fig. 8, the black circle represents the CH, and the node pointed by the arrow denotes the relay node. As expected from DACHER, the CHs in the hot-spot area are located near the centerline of each layer, and the MNs' data are collected. The CH of the non-hot-spot area is situated in the middle of the area to collect the data information of the MNs. Relay nodes are located near the centerline of the non-hot-spot area. The CHs transmit the collected data information to the relay node in the non-hot-spot area, and then, the relay node fuses the received data and delivers it to the other relay node in the upper layer or CH. Then, it passes all the data to the BS. In addition, the BS needs to play the role of the CH to collect the data information of the nodes in the first layer. Finally, the relay nodes establish a chain communication link from outside to inside with the CH of the hot-spot area, which can deliver all data to the BS.

2) Influence of the Number of Layers: In our layered approach, the sensing area is partitioned into concentric rings—each ring representing a defined radial interval from the BS—which enables a more localized selection of CHs and reduces competition among distant nodes. As we increment the number of layers, the network topology becomes more finely grained, allowing for improved balance in cluster sizes and more precise relay placement in outer rings. However, increasing the number of layers also entails higher administrative overhead, as each additional ring boundary must be delineated and managed. Empirically, we observe that well-chosen values of this layer count confer longer node survival times and mitigate energy hot spots, as each ring carries a proportionate share of the forwarding workload. Conversely, too few rings

can lead to uneven energy dissipation when nodes of different distances from the BS are grouped. Overall, a moderate layer count ($I = 6$) provides the best tradeoff, distributing CH responsibilities more effectively while avoiding excessive complexity in updating and maintaining ring boundaries.

3) Influence of the Rotation Angle: The rotation angle β plays a critical role in the CH selection process of the DACHER protocol. Comparative simulation experiments were conducted following the approach in [37] to investigate its impact on network lifetime. The rotation angle was varied from 5° to 15° in increments of 1°. Evaluation metrics included the FND and LND rounds, as discussed in Section V-C.

The results, as illustrated in Fig. 9, reveal that β significantly affects network performance. When β is set to 13°, FND and LND achieve optimal values, resulting in the most extended network lifetime.

4) Influence of SN Number: The network scale of WSNs is an essential factor affecting network performance. If the network lifetime changes significantly with the number of sensors, it indicates that the adaptability and robustness of the routing protocol are poor. As shown in Table III, we have considered four simulation scenarios. For each scenario, we measure the influence of SN number on network lifetime. Here, the number of surviving nodes measures the network lifetime.

The simulation results, as illustrated in Fig. 10, demonstrate the performance of the DACHER protocol across different SN counts. Specifically, for SN values of 200, 350, 500, and 1000, the number of surviving nodes remains stable until approximately 1250 operational rounds. Furthermore, DACHER achieves network lifetimes of 2137, 2197, 2162, and 2048 rounds under these conditions. These findings indicate that DACHER exhibits strong adaptability and consistent performance even with significant variations in the number of sensor nodes.

As shown in Table V, the DACHER protocol exhibits markedly superior performance on key WSN metrics compared with the EOCGS [34], GNN [38], and CHHFO [39] protocols. In particular, DACHER achieves an FND value of 1039, which is significantly greater than those of EOCGS (641), GNN (592), and CHHFO (380). This finding indicates that DACHER effectively mitigates premature node failures during the initial operational phase of the network, thereby extending the stability period. A longer time from the start of network operation to the first node death implies that DACHER excels at balancing energy consumption across nodes, allowing the network to remain active for a more prolonged duration. Furthermore, DACHER attains a half node dead (HND) value of 1743, which surpasses the HND values reported by EOCGS (796), GNN (1125), and CHHFO (573). Maintaining a larger proportion of live nodes over an extended timeframe enhances data collection and transmission reliability, facilitating better coverage and accuracy in real-world WSN deployments.

Due to its balanced energy-consumption strategy, DACHER experiences fewer node deaths in the early network operation phase. Although the network unavoidably enters an IPL in the later phase, DACHER continues to sustain relatively high node activity. The delayed FND and HND values demonstrate that DACHER effectively prevents localized energy depletion, thus reducing the risk of early network fragmentation.

TABLE IV
EXPERIMENTAL PARAMETERS

Parameter	Value
E_0	0.5J
E_{elec}	50nJ/bit
ε_{fs}	10pJ/bit/m^2
ε_{mp}	0.0013pJ/bit/m^4
d_0	87m
r_0	15m
I	$I \geq 4$
Packet	4000bits
Z	4
β	$5° \leq \beta \leq 15°$
φ	$0 < \phi < 1$
C_1, C_2, C_3	$0 < C_i < 1, i = (1, 2, 3)$
θ	$0 \leq \theta \leq 1$
ω	2

In summary, DACHER maintains stable energy management and network coverage even in large-scale, high-density scenarios through its efficient clustering and hierarchical scheduling strategy. It demonstrates superior network lifetime and topological stability compared to benchmark protocols, achieving enhanced reliability, coverage efficiency, and communication performance.

5) Evaluation of Performance: In this section, we compare the indicators: the distribution of surviving, the number of alive nodes, the residual energy, and the network's lifetime. The protocols used in the comparative experiments are WLEACH-CK, LAR-CH, LBR-GWO, and CER-CH.

To ensure a comprehensive and equitable evaluation, DACHER is benchmarked against a carefully curated suite of hierarchical routing protocols that collectively span the state of the art. WLEACH-CK acts as a stringent LEACH-family baseline, employing weighted k-means clustering to represent an advanced evolution of the canonical scheme. LAR-CH and CER-CH serve as conceptual mirrors: the former allows an isolated assessment of rotation strategies, whereas the latter contrasts DACHER's flexible ring-and-sector framework with a rigid tree-based hierarchy. Finally, LBR-GWO introduces a meta-heuristic perspective, testing DACHER's competitiveness against optimizer-driven approaches. These benchmarks offer a broad and balanced cross section of contemporary solutions, enabling a rigorous appraisal of DACHER's relative strengths.

a) Comparison of the surviving nodes' distribution: Network topology is a key indicator that affects the network lifetime. Furthermore, the CH near BS undertakes more forwarding tasks and has an unpredictable impact on the network lifetime, which cannot be ignored. Therefore, the number of survival nodes around the BS is very critical. However, in most research on hierarchical routing protocols, network topology and energy level are not considered.

Fig. 11(a) and (b) illustrates the distribution of surviving and dead nodes in the DACHER protocol at different rounds. Specifically, Fig. 11(a) depicts the state of node survival at

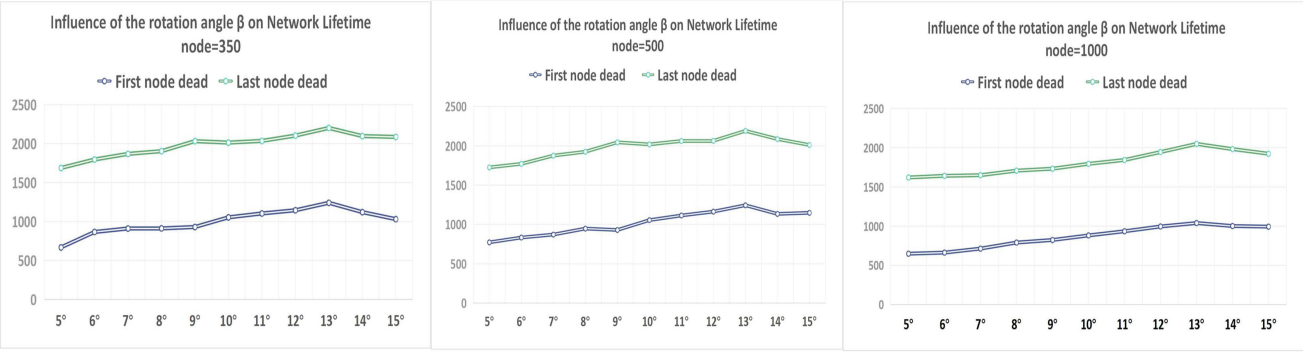

(a) (b) (c)

Fig. 9. Effect of β on death rounds. (a) Rotation angle (node = 350). (b) Rotation angle (node = 500). (c) Rotation angle (node = 1000).

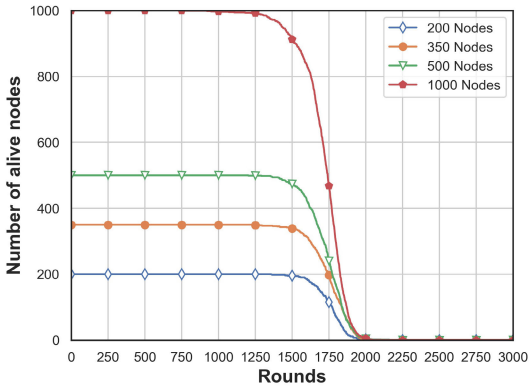

Fig. 10. Influence of SN number on the network lifetime.

the 500th round, where nodes near the BS remain operational. In contrast, Fig. 11(b) shows the state at the 1500th round, where a few nodes at the network's edge have turned red, indicating their failure. However, most nodes remain green, signifying that they are still active. Most failed nodes are located at the periphery, highlighting DACHER's effectiveness in maintaining a robust network topology.

To further demonstrate the superiority of DACHER and compare its performance against four other protocols, we focused on a 15 × 15 m^2 area centered around the BS. Using the Exp350 configuration, we simulated the percentage of surviving nodes in this area across the five protocols. The results, presented in Fig. 12, emphasize the significance of our contributions to network performance.

The simulation results reveal that at the 500th round, all five protocols maintain 100% node survival within the BS area, which persists until the 1000th round. Beyond 1000 rounds, the survival rates of the other four protocols decline significantly, with sharp drops by the 1500th round. In contrast, DACHER consistently achieves a survival rate exceeding 80% within the fixed range. This demonstrates that DACHER effectively mitigates node failures near the BS by optimizing cluster distribution, thereby preventing the formation of coverage holes and ensuring sustained network performance.

b) Comparison of alive nodes: The number of alive nodes is an indicator that directly reflects the performance of the DACHER. If the number of surviving nodes decreases faster, the network operational lifetime will be shorter, and the system can last less. Therefore, the number of alive nodes indicates the network lifetime. We suppose the same initial energy of the sensor and simulate the number of surviving nodes of the five protocols.

As illustrated in Fig. 13, the findings highlight the comparative effectiveness of the five protocols with respect to network lifetime. When the number of nodes in the WSN is 200, LBR-GWO experiences its first node failure at the 443rd round, after which the number of dead nodes increases rapidly. For WLEACH-CK, the first node failure occurs at the 862nd round, followed by a sharp decline in the number of surviving nodes. By the 1336th round, all nodes in WLEACH-CK had depleted their energy, while DACHER continues to operate with no node failures.

Notably, the other three algorithms maintain all nodes operational until the 1336th round. However, by the 2137th round, all protocols cease operation due to the BS losing connectivity with the network sensors. This trend is corroborated by additional figures, which further illustrate similar patterns.

The cumulative results highlight that DACHER consistently surpasses the other protocols, achieving over 2000 operational rounds under varying conditions. This underscores the strong adaptability and robustness of the DACHER protocol in maintaining network performance and prolonging network lifetime.

c) Comparison of residual energy: The distribution and number of surviving nodes are insufficient to evaluate the network performance. From the network's total energy perspective, energy consumption mainly comes from data transmission and signaling interaction. Therefore, it is necessary to simulate residual energy trends with total work rounds of five protocols. The simulation results are presented in Fig. 14.

Under the three experimental environments, the residual energy of the DACHER protocol has the slowest downward trend and the lowest energy-consumption rate. In addition, the residual energy of the WLEACH-CK protocol has the fastest energy-consumption rate.

Despite the increased number of sensors, which brings more complexity to energy imbalance, DACHER can still balance the energy consumption and make the consumption rate much slower than the other four protocols.

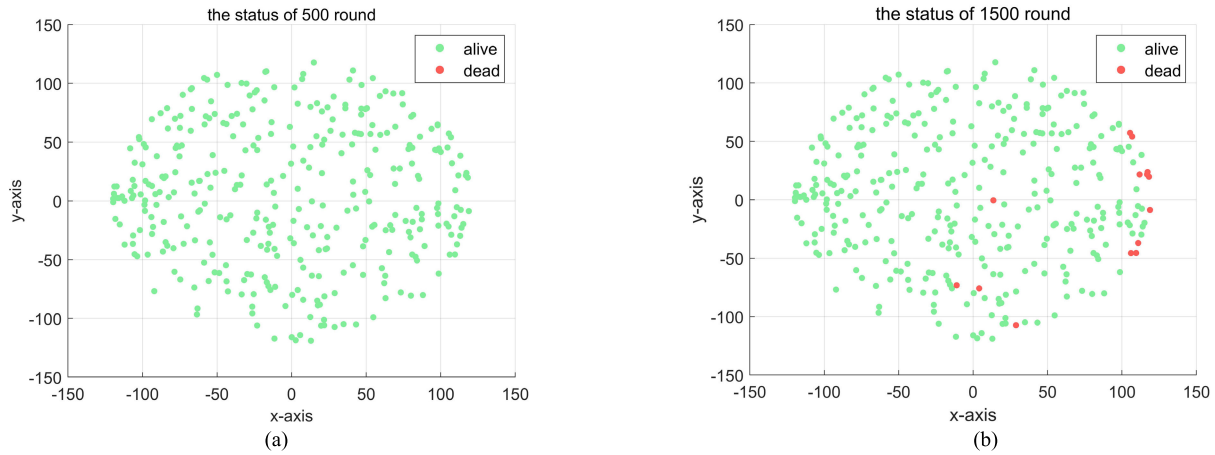

Fig. 11. Visualization of surviving and dead sensor nodes at different rounds for DACHER. (a) Alive (green color) and dead (red color) sensor nodes for DACHER after 500 *r*. (b) Alive (green color) and dead (red color) sensor nodes for DACHER after 1500 r.

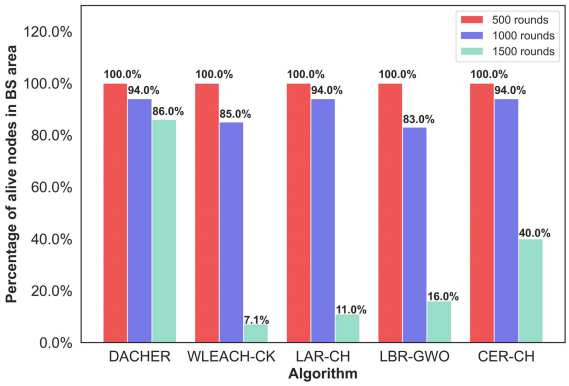

Fig. 12. Percentage of surviving nodes in the BS area.

d) Comparison of the stability period and network lifetime: The network lifetime can be divided into SPL and IPL; a reliable clustering protocol can shorten the IPL based on the long SPL.

As presented in Fig. 15, DACHER protocol maintains the network operational lifetime of 801, 417, 494, and 70 more than the WLEACH-CK, LAR-CH, LBR-GWO, and CER-CH for experiment Exp200, respectively. For a WSN scenario (Exp350), DACHER shows a longer lifetime of 700, 310, 600, and 344 more than WLEACH-CK, LAR-CH, LBR-GWO, and CER-CH, respectively. Also, when the network contains 1000 nodes (Exp1000), DACHER still gives a high value of over 2000 rounds compared with 1587, 1654, 1857, and 1945 rounds of WLEACH-CK, LAR-CH, LBR-GWO, and CER-CH, respectively. Simulated results show that DACHER maintains a high network lifetime value as the network size increases, indicating that DACHER works very well in large-scale WSNs.

Also, as shown in Fig. 16, it is deduced that DACHER has the longest SPL value for experiments Exp200 and Exp350. Notably, the SPL obtained in the DACHER protocol for Exp1000 is 96, 277, 516, and 368 rounds more than WLEACH-CK, LAR-CH, LBR-GWO, and CER-CH, respectively. The above results mean that the DACHER protocol can maintain stability in different scale networks.

The marked performance gains delivered by DACHER stem directly from its integrated temporal-and-spatial load-balancing design. The pronounced extension of the SPL in Fig. 16 originates from the proactive temporal balancing enforced by Algorithm 1: PR of the annular sectors continually redistributes the high-energy duty of CH service, thereby averting premature failure of any single node. This process is guided by the energy-aware CH-selection metric in (3) and (6), which preferentially assigns the role to nodes with greater residual energy.

The accompanying improvement in overall LND, as documented in Fig. 15, is chiefly a consequence of DACHER's spatial energy efficiency. Algorithm 2, together with the first-order radio model in (1), constructs chained intercluster transmission paths: long-haul links are replaced with a series of low-power short hops via relay nodes, sharply reducing per-round energy expenditure. This synergy—temporal balancing through rotation and spatial efficiency through relay chaining—underlies DACHER's consistent superiority across all evaluated metrics.

6) Summary of Results: Table VI illustrates the comparison of the network-lifetime gains obtained with DACHER against WLEACH-CK, LAR-CH, LBR-GWO, and CER-CH under three node-density settings (Exp200, Exp350, and Exp1000). From the sparse Exp200 scenario to the medium-density Exp350 scenario, DACHER consistently preserves a clear advantage. Even when the deployment is scaled to 1000 nodes within a 200 $\times$ 200 m^2 area (Exp1000), it still delivers the longest SPL. These results confirm that the protocol's RB layering and PR effectively equalize energy expenditure in both small and large networks, rendering DACHER resilient to premature energy depletion across a wide range of node densities.

Following the statistical significance analysis methodologies outlined in [40] and [41], the DACHER algorithm

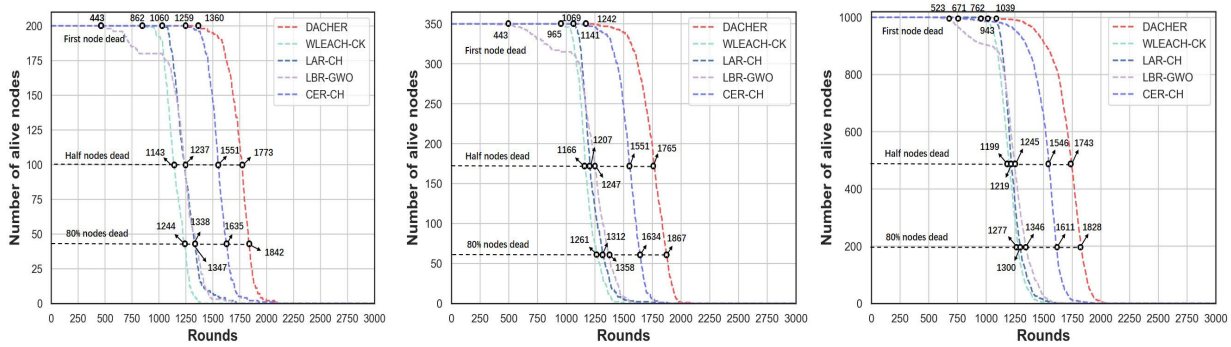

Fig. 13. Number of surviving nodes versus work rounds.

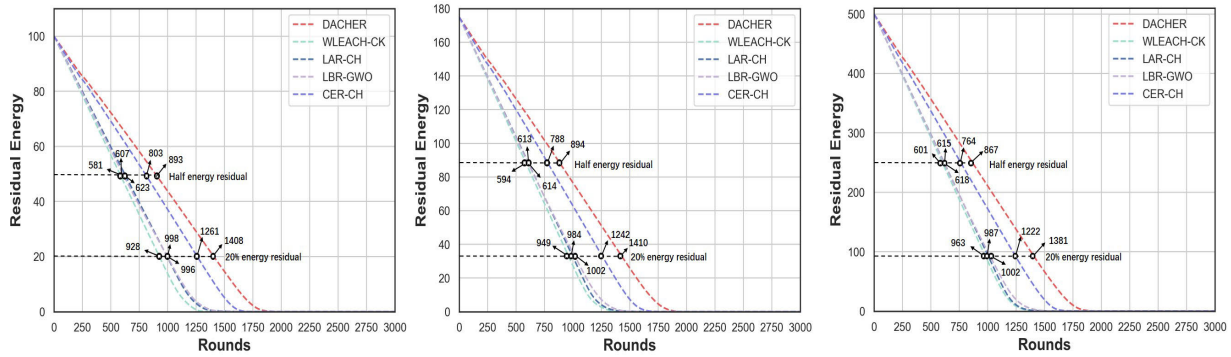

Fig. 14. Residual energy versus work rounds.

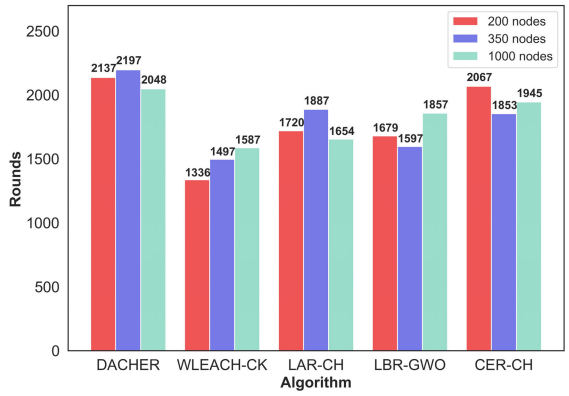

Fig. 15. Comparison of the network lifetime.

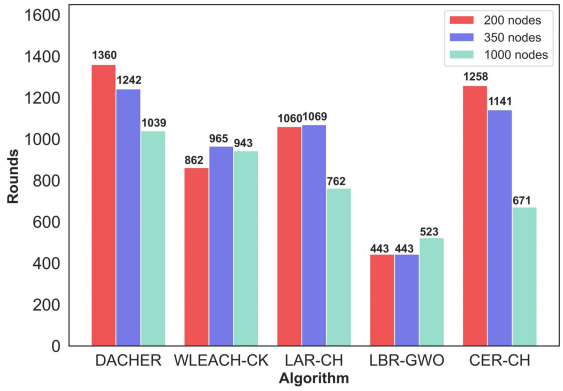

Fig. 16. Comparison of the SPL.

TABLE V
LIFETIME METRICS

Metrics	FND	HND	LND	SPL	IPL
EOCGS	641	796	823	641	182
GNN	592	1125	1156	592	564
CHHFO	380	573	689	380	309
DACHER	1039	1743	2048	1039	1009

was independently tested 20 times in two distinct deployment environments: 120 × 120 m^2 and 200 × 200 m^2. Table VII reports key statistical indicators related explicitly to network lifetime—including the mean, standard deviation, and confidence interval (CI)—to highlight the stability and robustness of DACHER under varying deployment scales.

E. Ablation Analysis of DACHER's Core Mechanisms

Our comparative results allow a quantitative analysis of DACHER's architectural contributions through a "natural ablation study." The performance metrics from the Exp350, as presented in Table VIII, effectively deconstruct the value of our innovations. As the data reveal, simply introducing an RB structure (as in LAR-CH) provides a substantial marginal gain (MG) of +390 rounds—a 26% lifetime improvement over the WLEACH-CK baseline. More importantly, DACHER's synergistic addition of systematic PR and RA hot-spot mitigation builds upon this foundation to deliver a further MG of +310 rounds, representing an additional 16% increase in network longevity. This clear, stepwise improvement empirically validates our core thesis: while a structured topology is beneficial,

TABLE VI
PERFORMANCE COMPARISON OF WLEACH-CK, LAR-CH, LBR-GWO, CER-CH, AND DACHER

Environment	Protocols	FND	LND	SPL	IPL
Exp200 120 x 120 m^2	WLEACH-CK	862	1336	862	474
	LAR-CH	1060	1720	1060	660
	LBR-GWO	443	1679	443	1236
	CER-CH	1259	2067	1259	808
	DACHER	1360	2137	1360	777
Exp350 120 x 120 m^2	WLEACH-CK	965	1497	965	532
	LAR-CH	1069	1887	1069	818
	LBR-GWO	443	1597	443	1154
	CER-CH	1141	1853	1141	712
	DACHER	1242	2197	1242	955
Exp1000 200 x 200 m^2	WLEACH-CK	943	1587	943	644
	LAR-CH	762	1654	762	892
	LBR-GWO	523	1857	523	1334
	CER-CH	671	1945	671	1274
	DACHER	1039	2048	1039	1009

TABLE VII
STATISTICAL SIGNIFICANCE ANALYSIS OF DACHER PERFORMANCE

Environment	Mean	Standard Deviation	Standard Error	95% Confidence Interval
Exp350 120 x 120 m^2	1796.6	191.50	42.82	[1706.97, 1886.23]
Exp1000 200 x 200 m^2	1655.4	218.01	48.75	[1553.32, 1757.38]

TABLE VIII
NATURAL ABLATION ANALYSIS IN EXP350

Protocols	RB	PR	RA	LND	MG
WLEACH-CK	✗	✗	✗	1497	–
LAR-CH	✓	✗	✗	1887	+390 rounds
DACHER	✓	✓	✓	2197	+310 rounds

it is the active and dynamic management of both temporal and spatial loads that are critical for maximizing the lifetime of large-scale WSNs.

VI. CONCLUSION AND FUTURE WORK

In this work, we introduced DACHER, a low-resource consumption dynamic area CH election routing protocol to enhance energy balance and extend network lifetime in large-scale WSNs. By annularly layering the sensing region around the BS, DACHER effectively controls the number and placement of CHs and allocates relay nodes to create a chain-based intercluster path from the outermost to the innermost layers. This design simultaneously minimizes both intracluster and intercluster energy overhead. Furthermore, through PR of clustered zones—governed by parameters such as node residual energy, rotation angle, and annular layers with specified layer intervals and layer counts—the protocol continuously redistributes the communication load, thereby mitigating single-point failures. Extensive simulations show that DACHER surpasses state-of-the-art hierarchical protocols—WLEACH-CK, LAR-CH, LBR-GWO, and CER-CH—across network sizes from 200 to 1000 nodes. Specifically, in a 1000-node deployment, DACHER delivers the most extended network lifetime and stability period, reaching an LND of 2048 rounds and boosting FND by 96–516 rounds relative to the baselines. These gains translate into lifetime improvements of up to 29.0%, underscoring DACHER's effectiveness in forestalling premature energy depletion. The quantitative evidence highlights DACHER's advantages in energy efficiency, longevity, and load balancing for large-scale WSNs. Nonetheless, the current design presumes static nodes and does not accommodate mobility; future work will, therefore, investigate the following avenues.

1) *Fault-Tolerant and Topology-Aware Adaptation:* Extend DACHER to operate in heterogeneous and dynamic environments. This involves developing topology-aware mechanisms that adapt to nonuniform node deployments while providing fault tolerance. Such a system would autonomously detect and reroute traffic around failed CHs or relay nodes, ensuring network resilience for mission-critical applications.
2) *Mobility-Aware Heterogeneity Enhancement:* Integrate realistic random and group mobility models (e.g., unmanned aerial vehicle (UAV) networks) into the DACHER evaluation framework to rigorously quantify CH selection stability, reclustering overhead, latency, and throughput under heterogeneous, dynamically changing topologies.
3) *Security Integration:* Integrate robust security mechanisms into DACHER to enhance confidentiality and integrity while minimizing additional overhead, ensuring secure data communication in WSNs [42], [43].
4) *AI-Driven Optimization With TinyML:* Investigate a artificial intelligence (AI)-augmented version of DACHER, combining geometry-based rotation with a TinyML-optimized policy module to enable on-device learning within the constraints of Telos-B-class nodes.

REFERENCES

[1] W. Choi, J. Kim, S. Lee, and E. Park, "Smart home and Internet of Things: A bibliometric study," *J. Cleaner Prod.*, vol. 301, Jun. 2021, Art. no. 126908.
[2] H. Verma, N. Chauhan, and L. K. Awasthi, "A comprehensive review of 'Internet of Healthcare Things': Networking aspects, technologies, services, applications, challenges, and security concerns," *Comput. Sci. Rev.*, vol. 50, Nov. 2023, Art. no. 100591.
[3] W. S. Kiran, A. J. Wilson, and A. S. Radhamani, "Spiking quantum fire hawk network based reliable scheduling for lifetime maximization of wireless sensor network," *Trans. Emerg. Telecommun. Technol.*, vol. 35, no. 11, Nov. 2024, Art. no. e70019.
[4] S. Mumtaz, A. Al-Dulaimi, V. Frascolla, S. A. Hassan, and O. A. Dobre, "Guest editorial special issue on 5G and beyond—Mobile technologies and applications for IoT," *IEEE Internet Things J.*, vol. 6, no. 1, pp. 203–206, Feb. 2019.
[5] M. Cui et al., "Secure data sharing for consortium blockchain-enabled vehicular social networks," *IEEE Trans. Veh. Technol.*, vol. 73, no. 12, pp. 19682–19695, Dec. 2024.
[6] X. Yang, J. Yan, D. Wang, Y. Xu, and G. Hua, "WOAD3QN-RP: An intelligent routing protocol in wireless sensor networks—A swarm intelligence and deep reinforcement learning based approach," *Expert Syst. Appl.*, vol. 246, Jul. 2024, Art. no. 123089.

[7] L. Zhang, X. Li, F. Wei, and Y. Li, "RETRACTED: Indoor 3-D localization based on simulated annealing bat algorithm," *Int. J. Electr. Eng. Educ.*, vol. 60, no. 1, pp. 3261–3278, Oct. 2023.

[8] C. Tang and D. Han, "A low resource consumption clone detection method for multi-base station wireless sensor networks," *IEEE Access*, vol. 8, pp. 128349–128361, 2020.

[9] A. Benelhouri, H. Idrissi-Saba, and J. Antari, "An evolutionary routing protocol for load balancing and QoS enhancement in IoT enabled heterogeneous WSNs," *Simul. Model. Pract. Theory*, vol. 124, Apr. 2023, Art. no. 102729.

[10] Z. Wang, W. Zeng, S. Yang, D. He, and S. Chan, "UCRTD: An unequally clustered routing protocol based on multihop threshold distance for wireless sensor networks," *IEEE Internet Things J.*, vol. 11, no. 17, pp. 29001–29019, Sep. 2024.

[11] P. Sharma, M. Sharma, R. Singh, V. Kumar, R. Agarwal, and P. K. Malik, "NHARSO-IWSN: A novel hybridized adaptive-network-based fuzzy inference system with reptile search optimization algorithm-based routing protocol for Internet of Things-enabled wireless sensor networks," *IEEE Trans. Consum. Electron.*, vol. 70, no. 3, pp. 6293–6302, Aug. 2024.

[12] N. Sirdeshpande and V. Udupi, "Fractional lion optimization for cluster head-based routing protocol in wireless sensor network," *J. Franklin Inst.*, vol. 354, no. 11, pp. 4457–4480, Jul. 2017.

[13] S. M. Bozorgi, A. Shokouhi Rostami, A. A. R. Hosseinabadi, and V. E. Balas, "A new clustering protocol for energy harvesting-wireless sensor networks," *Comput. Electr. Eng.*, vol. 64, pp. 233–247, Nov. 2017.

[14] R. Pachlor and D. Shrimankar, "LAR-CH: A cluster-head rotation approach for sensor networks," *IEEE Sensors J.*, vol. 18, no. 23, pp. 9821–9828, Dec. 2018.

[15] R. Chen, Y. Zhang, Y. Fei, and P. Kar, "WLEACH-CK: Weighted K-means based LEACH-C algorithm for cluster head selection," in *Proc. 17th Int. Conf. Design Reliable Commun. Netw. (DRCN)*, Apr. 2021, pp. 1–6.

[16] R. T. Al-Zubi, N. Abedsalam, A. Atieh, and K. A. Darabkh, "LBCH: Load balancing cluster head protocol for wireless sensor networks," *Informatica*, vol. 29, no. 4, pp. 633–650, Jan. 2018.

[17] N. Moussa, Z. Hamidi-Alaoui, and A. El Belrhiti El Alaoui, "ECRP: An energy-aware cluster-based routing protocol for wireless sensor networks," *Wireless Netw.*, vol. 26, no. 4, pp. 2915–2928, May 2020.

[18] P. Rawat and S. Chauhan, "Probability based cluster routing protocol for wireless sensor network," *J. Ambient Intell. Humanized Comput.*, vol. 12, no. 2, pp. 2065–2077, Feb. 2021.

[19] M. Micheletti, L. Mostarda, and A. Navarra, "CER-CH: Combining election and routing amongst cluster heads in heterogeneous WSNs," *IEEE Access*, vol. 7, pp. 125481–125493, 2019.

[20] S. Kaur, R. N. Mir, A. Khamparia, P. Rani, D. Gupta, and A. Khanna, "Heterogeneous load balancing clustering protocol for wireless sensor networks," *Cognit. Syst. Res.*, vol. 70, pp. 10–17, Dec. 2021.

[21] J. Hou, J. Qiao, and X. Han, "Energy-saving clustering routing protocol for wireless sensor networks using fuzzy inference," *IEEE Sensors J.*, vol. 22, no. 3, pp. 2845–2857, Feb. 2022.

[22] S. Murugaanandam and V. Ganapathy, "Reliability-based cluster head selection methodology using fuzzy logic for performance improvement in WSNs," *IEEE Access*, vol. 7, pp. 87357–87368, 2019.

[23] C. Naik and P. D. Shetty, "FLAG: Fuzzy logic augmented game theoretic hybrid hierarchical clustering algorithm for wireless sensor networks," *Telecommun. Syst.*, vol. 79, no. 4, pp. 559–571, Apr. 2022.

[24] A. A. Baradaran and K. Navi, "HQCA-WSN: High-quality clustering algorithm and optimal cluster head selection using fuzzy logic in wireless sensor networks," *Fuzzy Sets Syst.*, vol. 389, pp. 114–144, Jun. 2020.

[25] A. Ali et al., "Enhanced fuzzy logic zone stable election protocol for cluster head election (E-FLZSEPFCH) and multipath routing in wireless sensor networks," *Ain Shams Eng. J.*, vol. 15, no. 2, Feb. 2024, Art. no. 102356.

[26] J. Wang, N. Wang, H. Wang, K. Cao, and A. M. El-Sherbeeny, "GCP: A multi-strategy improved wireless sensor network model for environmental monitoring," *Comput. Netw.*, vol. 254, Dec. 2024, Art. no. 110807.

[27] D. Han, N. Pan, and K.-C. Li, "A traceable and revocable ciphertext-policy attribute-based encryption scheme based on privacy protection," *IEEE Trans. Dependable Secure Comput.*, vol. 19, no. 1, pp. 316–327, Jan. 2022.

[28] J. John and P. Rodrigues, "MOTCO: Multi-objective Taylor crow optimization algorithm for cluster head selection in energy aware wireless sensor network," *Mobile Netw. Appl.*, vol. 24, no. 5, pp. 1509–1525, Oct. 2019.

[29] B. Dwivedi, B. D. K. Patro, V. Srivastava, and S. S. Jadon, "LBR-GWO: Layered based routing approach using grey wolf optimization algorithm in wireless sensor networks," *Concurrency Comput., Pract. Exper.*, vol. 34, no. 4, Feb. 2022, Art. no. e6603.

[30] Y. Liu, H. Huang, and J. Zhou, "A dual cluster head hierarchical routing protocol for wireless sensor networks based on hybrid swarm intelligence optimization," *IEEE Internet Things J.*, vol. 11, no. 9, pp. 16710–16721, May 2024.

[31] A. Panchal and R. K. Singh, "EEHCHR: Energy efficient hybrid clustering and hierarchical routing for wireless sensor networks," *Ad Hoc Netw.*, vol. 123, Dec. 2021, Art. no. 102692.

[32] R. K. Singh, S. Verma, A. Panchal, and S. K. Dubey, "Modified RCH-LEACH (MRCH) for wireless sensor networks (WSN)," in *Proc. 9th Int. Congr. Inf. Commun. Technol.*, in Lecture Notes in Networks and Systems, X. S. Yang, S. Sherratt, N. Dey, and A. Joshi, Eds., Singapore: Springer, Jan. 2024, pp. 331–340.

[33] A. Panchal and R. K. Singh, "EOCGS: Energy efficient optimum number of cluster head and grid head selection in wireless sensor networks," *Telecommun. Syst.*, vol. 78, no. 1, pp. 1–13, Sep. 2021.

[34] F. Sun, S. Wang, C. Zhang, and H. Zhang, "Clustering of unknown protocol messages based on format comparison," *Comput. Netw.*, vol. 179, Oct. 2020, Art. no. 107296.

[35] A. Ouyang, Y. Lu, Y. Liu, M. Wu, and X. Peng, "An improved adaptive genetic algorithm based on DV-hop for locating nodes in wireless sensor networks," *Neurocomputing*, vol. 458, pp. 500–510, Oct. 2021.

[36] N. Ma, H. Zhang, H. Hu, and Y. Qin, "ESCVAD: An energy-saving routing protocol based on Voronoi adaptive clustering for wireless sensor networks," *IEEE Internet Things J.*, vol. 9, no. 11, pp. 9071–9085, Jun. 2022.

[37] J. Wang, Z. Du, Z. He, and X. Wang, "A cluster-head rotating election routing protocol for energy consumption optimization in wireless sensor networks," *Complexity*, vol. 2020, pp. 1–13, Dec. 2020.

[38] M. Saadati, S. M. Mazinani, A. A. Khazaei, and S. J. S. M. Chabok, "Energy efficient clustering for dense wireless sensor network by applying graph neural networks with coverage metrics," *Ad Hoc Netw.*, vol. 156, Apr. 2024, Art. no. 103432.

[39] L. Yang, D. Zhang, L. Li, and Q. He, "Energy efficient cluster-based routing protocol for WSN using multi-strategy fusion snake optimizer and minimum spanning tree," *Sci. Rep.*, vol. 14, no. 1, Jul. 2024, Art. no. 16786.

[40] R. P. S. Hada and A. Srivastava, "Dynamic cluster head selection in WSN," *ACM Trans. Embedded Comput. Syst.*, vol. 23, no. 4, pp. 1–27, Jul. 2024.

[41] M. Kingston Roberts, P. Ramasamy, and F. Dahan, "An innovative approach for cluster head selection and energy optimization in wireless sensor networks using zebra fish and sea horse optimization techniques," *J. Ind. Inf. Integr.*, vol. 41, Sep. 2024, Art. no. 100642.

[42] D. Han, Y. Zhu, D. Li, W. Liang, A. Souri, and K.-C. Li, "A blockchain-based auditable access control system for private data in service-centric IoT environments," *IEEE Trans. Ind. Informat.*, vol. 18, no. 5, pp. 3530–3540, May 2022.

[43] J. Li, D. Han, T.-H. Weng, H. Wu, K.-C. Li, and A. Castiglione, "A secure data storage and sharing scheme for port supply chain based on blockchain and dynamic searchable encryption," *Comput. Standards Inter.*, vol. 91, Jan. 2025, Art. no. 103887.

Xiaohu Huang received the master's degree from the School of Information Engineering, Shanghai Maritime University, Shanghai, China, in 2021.

Bing Han received the B.S. and Ph.D. degrees from the Department of Electrical Engineering, Dalian University of Technology, Dalian, China, in 2003 and 2009, respectively.

He is currently a Researcher with the State Key Laboratory of Navigation and Safety Technology, Shanghai Ship and Shipping Research Institute Company Ltd., Shanghai, China. He has authored or co-authored over 60 journal articles and conference papers.

Dezhi Han (Senior Member, IEEE) received the Ph.D. degree from the Huazhong University of Science and Technology, Wuhan, China, in 2005.

He is currently a Professor of Computer Science and Engineering with Shanghai Maritime University, Shanghai, China. His research interests include cloud computing, mobile networking, wireless communication, and cloud security.

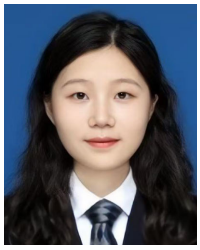

Ruyue Zhang received the master's degree from the School of Information Engineering, Shanghai Maritime University, Shanghai, China, in 2022.

Kuan-Ching Li (Senior Member, IEEE) received the Ph.D. degree from the University of São Paulo, São Paulo, Brazil, in 2001.

He is currently a Life Distinguished Professor with Providence University, Taichung, Taiwan, where he is also the Director of the High-Performance Computing and Networking Center, established through collaborations with industry. Besides publishing articles in renowned journals and conferences, he is a co-author/co-editor of more than 50 books published by well-known publishers. His research interests include big data, parallel and distributed computing, and emerging technologies.

Dr. Li is a Fellow of IET and a member of AAAS.